Polymeric Pseudo Crown Ether for Cation Recognition via Cation Template-Assisted Cyclopolymerization

Takaya Terashima, Minami Kawabe, Yuichiro Miyabara, Hiroaki Yoda, Mitsuo Sawamoto*
*Corresponding Author
Department of Polymer Chemistry, Graduate School of Engineering, Kyoto University,
Katsura, Nishikyo-ku, Kyoto 615-8510, JAPAN
Tel: +81-75-383-2600, Fax: +81-75-383-2601
E-mail: sawamoto@star.polym.kyoto-u.ac.jp

Abstract

Cyclopolymerization is a chain polymerization of bifunctional monomers via alternating process of intramolecular cyclization and intermolecular addition, to give soluble linear polymers consisting of in-chain cyclic structures. Though cyclopolymers comprising in-chain multiple large rings potentially show unique functions, they generally involve the elaborate design of bifunctional monomers. Herein, we report cation template-assisted cyclopolymerization of poly(ethylene glycol) dimethacrylates as an efficient strategy to directly lead to polymeric pseudo-crown ethers with large in-chain cavities (up to 30 membered rings) for selective molecular recognition. The key is to select a size-fit metal cation for the spacer unit of the divinyl monomers to form a pseudo-cyclic conformation, where the two vinyl groups are suitably positioned for intramolecular cyclization. The marriage of supramolecular chemistry and polymer chemistry affords efficient, one-pot chemical transformation from common chemical reagents with simple templates to functional cyclopolymers.

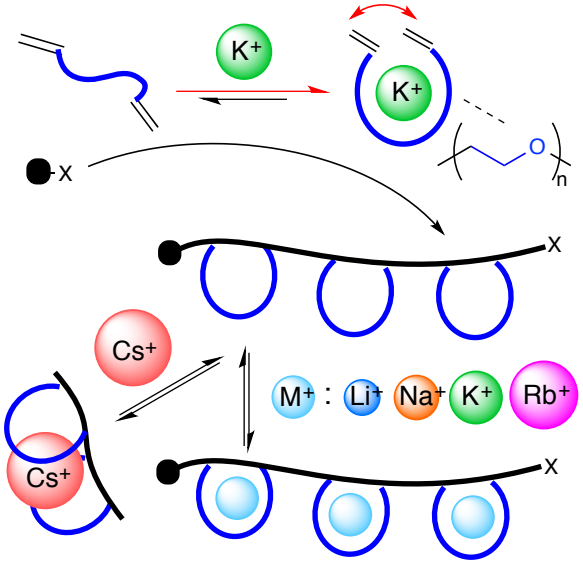

Introduction

The marriage of supramolecular/organic chemistry and polymer chemistry is a promising strategy for the efficient and selective synthesis of designed materials.[1-3] It often involves template molecules that non-covalently or covalently interact with substrates, to induce a specific conformation, in which reactive sites and substrates are oriented suitably for chemical bond formation. For example, such a template-directed synthesis[4-10] utilizing supramolecular interaction or molecular recognition is quite effective for intramolecular cyclization by bringing reactive sites close. Metal (M^+) or ammonium ($R_nNH_{4-n}^+$) cations are often employed as templates for selective cyclization of poly(ethylene glycol) (PEG)-containing substrates into crown ether derivatives[4,8] or interlocked molecules (rotaxanes and catenanes),[5-7,9,10] typically combined with metathesis reactions. Templates assist not only the selective production of such supramolecular materials[4-10] but also the precision control of primary structure of polymers.[11-18] For example, we and other groups have recently developed template-assisted precision control of tacticity[15] and monomer sequence[16-18] in conjunction with metal-catalyzed living radical polymerization.[19-22]

Cyclopolymerization[23-36] is a chain polymerization of bifunctional monomers via alternating propagation process of intramolecular cyclization and intermolecular addition, to give soluble linear polymers consisting of "in-chain" cyclic structures. This strategy affords direct and quantitative incorporation of cyclic units into polymers as repeating units, in sharp contrast to the polymerization of monomers bearing a cyclic pendent group[37] or the post-functionalization of linear polymers.[38] With the in-chain multiple cyclic units, cyclopolymers potentially show unique functions, e.g. polymeric (pseudo-)crown ethers recognize particular cations in a way different from monomeric counterparts.[25,32,39] The key for selective vinyl-type cyclopolymerization is of course to bring the two olefins in a bifunctional monomer to vicinity for effective intramolecular cyclization, so as to suppress intermolecular propagation with only one of the two alkene units into pendent olefin-bearing polymers; otherwise the dangling olefin further causes intermolecular crosslinking of polymers to give insoluble gels and/or branched polymers.[40-43] So far, cyclopolymers with relatively large in-chain rings (at most 20-membered rings) generally involved the elaborate design of bifunctional monomers that place two olefins close typically through a rigid spacer,[29-32] except for counterparts with small 5 or 6-membered rings from 1,6-dienes and 1,6-diynes.[33-36]

Herein, we report cation template-assisted controlled radical cyclopolymerization of poly(ethylene glycol) dimethacrylates [PEGnDMA: $CH_2=C(CH_3)COO–(CH_2CH_2O)_n–C(O)C(CH_3)=CH_2$, n = 4–8] as a novel, one-pot, and versatile strategy to selectively produce, so-called polymeric pseudo crown ethers, cyclopolymers with large in-chain PEG rings (each with 19 to 30-membered ether units, 13-100 rings per a chain) for

efficient and unique cation recognition (Fig. 1). The polymer synthesis is achieved through the specific interaction of the PEG unit with metal cation. Namely, PEGnDMA is treated with metal salts (M^+X^-) in polymerization to assume the pseudo-cyclic conformation (PEGnDMA-M^+) via dynamic equilibrium, where the two vinyl groups intramolecularly come adjacent and thereby suitably positioned for cycloaddition. The cyclization of PEGnDMA with a template was effective up to 30-membered "in-chain" PEG ring based on flexible eight oxyethyrene units. Typically, ruthenium-catalyzed polymerization of K^+-template PEG6DMA directly leads to water-soluble linear polymers with narrow MWDs (M_w/M_n ~ 1.2) and large 24-membered in-chain cyclic PEG units (>97 %), without gels nor unreacted dangling olefin. The cyclicPEG units efficiently work as nano cavities to interact with alkali metal cations, 1:1 per cyclic unit for Rb^+, K^+, Na^+, and Li^+ or 1:2 for Cs^+, and selectively recognize Na^+ over Li^+ or Bu_4N^+ and K^+ over Na^+ under competitive conditions. To our knowledge, this is the first example to apply cation templates for selective and efficient cyclopolymerization of divinyl monomers carrying a long, flexible spacer via the alternating propagation of intramolecular cyclization and intermolecular addition into cyclopolymers containing multiple and large in-chain PEG rings, in sharp contrast to conventional template-directed intramolecular cyclization for crown ether-based supramolecular materials.[4-10] It should be noted that this template-mediated cyclopolymerization is an efficient, one-pot, and selective chemical transformation from common reagents with simple templates to functional cyclopolymers.

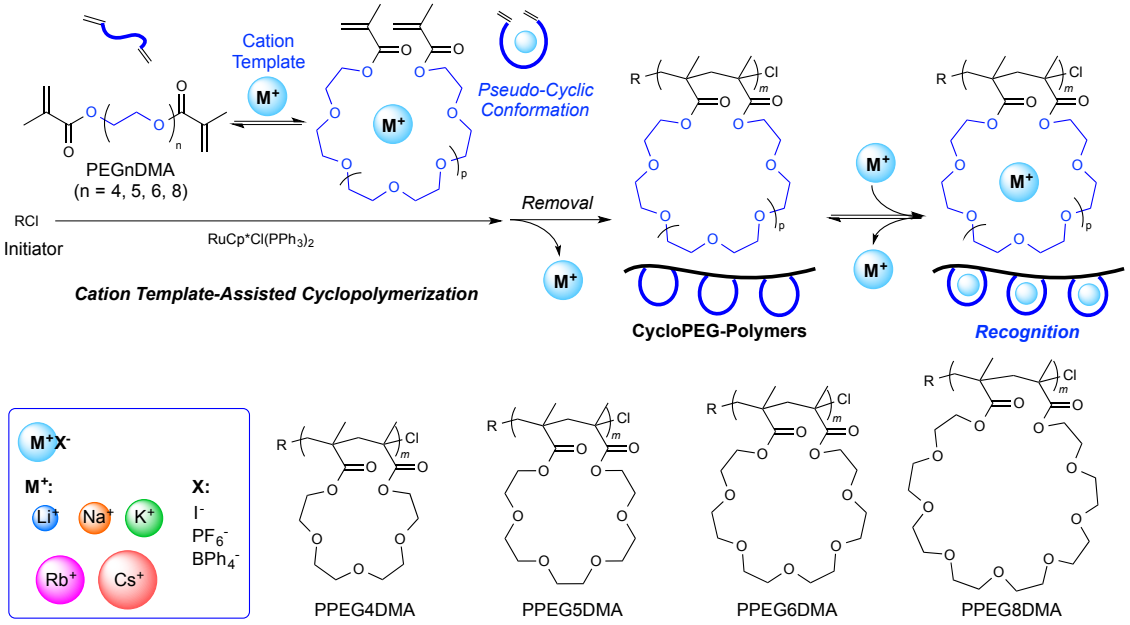

Figure 1: Cation template-assisted cyclopolymerization for polymeric pseudo crown ethers. Poly(ethylene glycol) dimethacrylate (PEGnDMA) efficiently interacts with metal cations to in situ form pseudo-cyclic conformation with the adjacent location of the two olefins, which induces the alternating propagation process of intramolecular cyclization and intermolecular addition to selectively give linear polymers comprising large in-chain cyclicPEG rings (up to 30 membered). Thus, cyclicPEG polymers behave as polymeric pseudo crown ethers to perform unique cation recognition dependent on the ring size.

Results

Cation template monomers. PEGnDMAs, dimethacrylates carrying a PEG spacer unit [–$(CH_2CH_2O)_n$–] of a well-defined degree of polymerization (n = 4, 5, 6, 8) were employed as monomers for cation template-assisted cyclopolymerization. The interaction between PEGnDMA and metal cations was first evaluated (Fig. 2, Supplementary Figs. S1-S3, Supplementary Table S1). In general, 18-crown-6, a cyclic crown ether consisting of six ethylene oxide units, efficiently recognizes potassium cation (K^+) because the inner pore is best fit in size for K^+.[4] PEG6DMA was thus mixed with KPF_6 in acetone-d_6/cyclohexanone (1/1, v/v) to analyze its interaction with K^+ by proton nuclear magnetic resonance spectroscopy (^{1}H NMR) (Fig. 2a,b). The protons (*c*, *d'*, and *d*) assignable to the PEG segment shifted to downfield by +0.04 ppm, larger than the accompanying shift in the chain-end methacrylate groups (*a*, *b*: < ~0.01 ppm), suggesting that the PEG spacer efficiently interacts with K^+. The stoichiometry of the interaction was 1:1 (one cation per

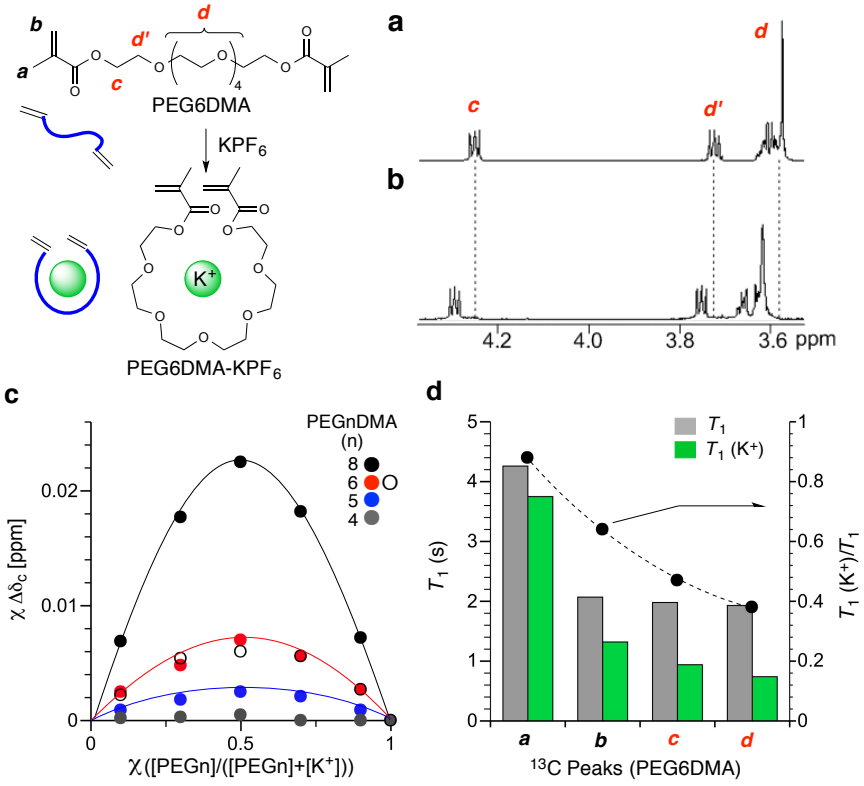

Figure 2: Interaction of poly(ethylene glycol) dimethacrylate (PEGnDMA) with a K template. ^{1}H NMR spectra of PEG6DMA (**a**) and PEG6DMA with KPF_6 (**b**) in acetone-d_6/cyclohexanone (1/1, v/v) at 30 °C. The proton signals of the ethylene oxide unit on PEG6DMA shifted to downfield in the presence of KPF_6. (**c**) Job plots obtained from PEGnDMAs with KI [filled circle: n = 4 (gray), 5 (blue), 6 (red), 8 (black)] or KPF_6 (n = 6: open black circle) by ^{1}H NMR spectroscopy ($[PEGnDMA]_0 + [K^+]_0$ = 10 mM). PEGnDMAs efficiently interact with K+ via 1:1 per the PEG unit, except for PEG4DMA. (**d**) Longitudinal relaxation time (T_1) measurements of the carbons for PEG6DMA (gray bar) and PEG6DMA with KPF_6 (green bar) by ^{13}C NMR. T_1 (K^+)s for PEG6DMA with KPF_6 turned smaller than those for PEG6DMA alone, meaning the decreasing mobility of PEG6DMA with K^+. Importantly, efficient interaction of the PEG segment (peaks: *c*, *d*) with K^+ was supported by the ratio [T_1 (K^+)/T_1: filled circle] for the PEG smaller than that for methacrylates (peaks: *a*, *b*).

PEG6DMA), as determined by the Job's method based on the chemical sift change of the PEG proton (peak *c*) and the molar fraction of PEG units (χ): [PEG6DMA]/[KPF_6] = 10/0–10/1, [PEG6DMA] + [KPF_6] = 10 mM (Fig. 2c); the plot showed a maximum at χ = 0.5. The association constant (K_a) was estimated as ~70M^{-1} by ^{1}H NMR titration experiment of PEG6DMA with K^+ (Supplementary Figs. S2 and S3, Supplementary Table S1). Similarly, PEG5DMA and PEG8DMA also captured K^+ via 1:1 interaction, whereas PEG4DMA was totally ineffective (Fig. 2c), suggesting that K^+ was suited for PEGnDMAs carrying 5 to 8 ethylene oxide units. In addition, PEG6DMA recognized K^+ more efficiently than Na^+ and Li^+ (NaI: K_a = ~30 M^{-1}; LiI: no specific interaction, Supplementary Table S1).

The local mobility of PEG6DMA was further evaluated with longitudinal relaxation time (T_1) of the carbons (*a–d*) in the presence of KPF_6 by ^{13}C NMR ([PEG6DMA]/[KPF_6] = 1/2; Fig. 2d, Supplementary Fig. S4, Supplementary Table S2). For all the carbons, T_1s with K^+ [T_1 (K^+)s] were smaller than those without K^+ (T_1s). As plotted on Figure 2d, the ratio [T_1 (K^+)/T_1s] for PEG units (*c* and *d*) was much smaller than that for methacrylate moieties (*a* and *b*), demonstrating that the PEG segment predominantly binds K^+. The same conclusion was also supported by UV-vis analysis (Supplementary Fig. S5).

Template-assisted cyclopolymerization. Cation template-assisted cyclopolymerization of PEG6DMA was carried out in conjunction with a ruthenium catalytic system [$RuCp^*Cl(PPh_3)_2$/*n*-Bu_3N] and a chloride initiator [H-$(MMA)_2$-Cl][44] in cyclohexanone at 40 °C. Following the cation recognition data, the bifunctional monomer was mixed with K^+ at 1/1 molar ratio in cyclohexanone to in situ transform a pseudo-cyclic monomer with K^+ template. Without further isolation of the complex, the mixture was directly polymerized under dilute conditions ([PEG6DMA]$_0$ = 25–100 mM) (Fig. 3, Table 1, Supplementary Fig. S6). The targeted degree of polymerization (*DP* = [PEG6DMA]$_0$/[H-$(MMA)_2$-Cl]$_0$) was set at 12.5–100, i.e. the number of "in-chain" cyclic units per polymer = 12.5, 25, 50, and 100. The polymerization smoothly and homogeneously proceeded in high yield (~90 % conversion in 30 – 56 h) without any gelation, independent of the targeted *DP*. The number-average molecular weight of products increased with increasing conversion and was proportional to the targeted *DP*s [M_n = 7500 – 31100; M_w/M_n = 1.1 - 1.5; by size-exclusion chromatography (SEC); Fig. 3a]. Thus, this ruthenium-mediated cyclopolymerization with metal cation templates was efficiently controlled to lead to linear polymers. Such a fine control was also maintained with excess cation over the monomer ([PEG6DMA]$_0$/[KPF_6]$_0$ = 1/1, 1/2, 1/5; *DP* = 12.5; M_w/M_n = <1.2). In contrast, direct polymerization of PEG6DMA in a cation-free system (entries 1,7) was retarded and resulted in high molecular weight products with bimodal distribution (M_w/M_n: ~ 2.0) and/or some gels, suggesting

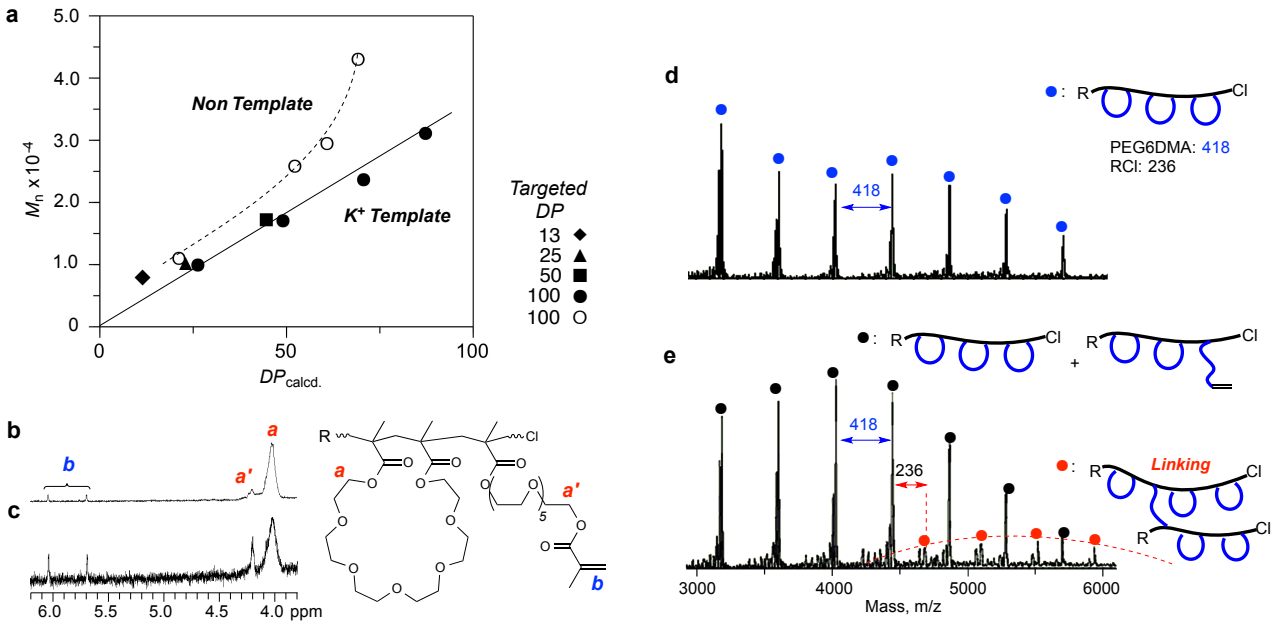

Figure 3: K^+ template-assisted cyclopolymerization of hexaethylene glycol dimethacrylate (PEG6DMA). (**a**) Number-averaged molecular weight as a function of calculated degree of polymerization ($DP_{calcd.}$): [PEG6DMA]/[KPF_6]/[H-$(MMA)_2$-Cl (RCl)]/[$RuCp^*Cl(PPh_3)_2$]/[*n*-Bu_3N] = 25-100/0-100/2.0, 1.0/0.5/20 mM in cyclohexanone at 40 °C. ^1H NMR (**b**,**c**) and MALDI-TOF-MS (**d**,**e**) spectra of initial PPEG6DMA samples (*Targeted DP* = 13) obtained with a KPF_6 template (**b**,**d**) and without the template (**c**,**e**). The K^+ template-assisted polymerization of PEG6DMA smoothly and selectively gave linear PPEG6DMA with high cyclization efficiency (>97%, **d**: filled blue circle), whereas the direct polymerization of PEG6DMA induced intermolecular linking reaction of polymer chains to lead to high molecular weight products including dangling olefins (~20%, **e**: filled black and red circles).

intermolecular cross-linking of linear chains.

Microscopic structures of products were analyzed by matrix-assisted laser desorption ionization time-of-flight mass (MALDI-TOF-MS) spectrometry and ^1H NMR spectroscopy, to determine intramolecular cyclization efficiency (CE).[18] Figure 3d shows a typical MALDI spectrum of poly(PEG6DMA) obtained with K^+ at the initial stage (targeted *DP* = 12.5; ~30 % conversion in entry 2). The sample exhibited a single series of peaks (blue filled circle), regularly separated by the molar mass of the monomer (418.5). The absolute mass of each peak was equal to that expected for the PEG6DMA polymer capped with one initiator fragment [H–$(MMA)_2$–] at the α-end and one chlorine at the ω-end [cf. m/e for H–$(MMA)_2$– + Cl: 236.7], plus a sodium ion from externally added salt for ionization. The products showed ^1H NMR signals of the methacrylate backbone (CH_3-: 0.7 – 1.2 ppm; -CH_2-: 1.4 – 2.0 ppm) and the cyclized PEG units (-CH_2CH_2O-: 3.4 – 3.7 ppm; -$COOCH_2CH_2O$- (***a***+***a'***: 4.0 – 4.2 ppm) but virtually without olefin signals (***b***: 5.7, 6.0 ppm) (Fig. 3b, Supplementary Fig. S7). From the signal intensity ratio ***b***/(***a***+***a'***), the dangling (unreacted) olefin content was estimated as 4.9% for an initial sample (conversion =

~30 %, Fig. 3b) and 2.4 % for a final sample (conversion 87%, Supplementary Fig. S7). The decrease with conversion suggests that the observed olefin might be located at the ω-terminal unit, where one methacrylate in the monomer is consumed by intermolecular propagation, while another stands by for intramolecular cyclization.

Table 1: K^+ template-assisted cyclopolymerization of PEGnDMA.[a]

Entry	PEG (**n**)	*DP*	PEG/KPF_6	Time (h)	Conv.[b] (%)	M_n[c]	M_w/M_n[c]	CE[d] (%) (olefin/linking)	Gel[f]	*mm*/*mr*/*rr*[g]
1	6	12.5	1/0	156	84	3600	1.24	- (20/+)	+	-
2	6	12.5	1/1	56	87	7500	1.11	95 (5/-), 98 (2/-)[e]	-	-
3	6	12.5	1/2	45	90	7900	1.20	92 (8/-), 99 (1/-)[e]	-	2.5/41.0/56.4
4	6	12.5	1/5	34	93	7900	1.10	96 (4/-), 98 (2/-)[e]	-	-
5	6	25	1/1	34	93	10200	1.23	96 (4/-)	-	-
6	6	50	1/1	30	90	17200	1.40	96 (4/-)	-	-
7	6	100	1/0	192	69	42900	1.89	- (9/+)	-	-
8	6	100	1/1	30	87	31100	1.56	97 (3/-), 99 (1/-)[e]	-	-
9	4	12.5	1/2	70	85	7200	1.19	97 (3/-), 99 (1/-)[e]	-	1.3/29.2/69.5
10	5	12.5	1/2	98	93	8300	1.21	99 (1/-), 99 (1/-)[e]	-	2.2/35.6/62.2
11	8	12.5	1/0	292	71	15200	2.18	- (28/+)	+	-
12	8	12.5	1/2	70	87	8300	1.29	91 (9/-), 99 (1/-)[e]	-	2.9/36.6/60.5

[a] $[PEGnDMA]_0/[KPF_6]_0/[H\text{-}(MMA)_2\text{-}Cl\ (RCl)]_0/[RuCp^*Cl(PPh_3)_2]_0/[n\text{-}Bu_3N]_0$ = 25-100/0-125/1.0 or 2.0/0.5/20 mM in cyclohexanone at 40 °C; *DP* = $[PEGnDMA]_0/[RCl]_0$ = 25/2, 50/2, 100/2, 100/1 (mM/mM) = 12.5, 25, 50, 100.

[b] Determined by ^1H NMR with tetralin as an internal standard.

[c] M_n and M_w/M_n of final products: determined by SEC in DMF (10 mM LiBr) with PMMA standard calibration.

[d] Cyclization efficiency (CE), olefin (pendant olefin content), and linking (intermolecular linking of chains) for initial products (conv. = <30%). Olefin content: determined by ^1H NMR with the following equation: $100[4\boldsymbol{b}/(\boldsymbol{a} + \boldsymbol{a'})]$ (%) (peaks: see Fig. 3b,c). Linking: confirmed by MALDI-TOF-MS and/or SEC (high MW) (+: observed; -: not observed). CE for non-linking samples was calculated from the following: CE (%) = 100 – olefin.

[e] CE, olefin (pendant olefin content), and linking (intermolecular linking) for final products.

[f] Insoluble gel formed in reaction mixtures (+: observed; -: not observed).

[g] Stereoregularity of products was determined from the area ratio of carbonyl carbons of methacrylates by ^{13}C NMR.

These results indicate high CE (>97 %), i.e., nearly without intermolecular crosslinking, almost all methacrylate units of PEG6DMA are cyclopolymerized into linear cyclopolymers with a large 24-membered "in-chain" cyclic PEG units. Separate experiments also showed that CE was as high as 95–99 %, invariably independent of the template feed ($[PEG6DMA]_0/[KPF_6]_0$ = 1/1 – 1/5) and targeted *DP* ($[PEG6DMA]_0/[initiator]_0$ = 12.5-100).

On the contrary, samples prepared without K^+ showed two series of mass peaks from the initial stage of the polymerization (~ 30 % conversion in entry 1; Fig. 3e). In addition to a series for cyclopoly(PEG6DMA) with one α-end initiator fragment (black filled circles), another series in

higher molecular weight region (red filled circles) was consistent with polymers carrying two initiator fragments indicative of intermolecular crosslinking (coupling) of two chains. These samples showed large ^{1}H NMR signals of dangling olefins (***b***) and adjacent methylene units (***a'***) (Fig. 3c), in which, without cation template, ca. 20 % monomer units were not intramolecularly cyclized even under diluted monomer conditions (25 mM).

We further examined cyclopolymerization with other templates ($LiPF_6$, $NaPF_6$, and $CsBPh_4$) and/or PEG dimethacrylate monomers of different spacer length (PEGnDMA; n = 4, 5, 8) (Table1, Supplementary Table S3, Supplementary Figs. S8). For PEG6DMA, KPF_6 (K^+) was the most effective template; CE: 85 % ($LiPF_6$), 93 % ($NaPF_6$), 95 % (KPF_6), 85 % ($CsBPh_4$); < 80 % (no template)]. Random and block copolymerizations with methyl methacrylate (MMA) were also possible [random: MMA/PEG6DMA = 25/13 or 75/13; M_w/M_n = 1.2; block (from MMA): MMA/PEG6DMA = 100/13; M_w/M_n = 1.3] (Supplementary Figs. S9 and 10). The K^+ template was also applicable to PEG5DMA and PEG8DMA to give linear cyclopolymers carrying 21- and 30-membered in-chain PEG rings, respectively (cf. 24-membered rings with PEG6DMA). In contrast, the cyclopolymerization of PEG4DMA occurred in fairly high CE independent of templates (even without a template cation), because the restricted conformation from the relatively short spacer renders the two vinyl groups intramolecularly close to each other without assistance of a template.[28,43]

The template effect on the conformation of PEGnDMA/K^+ pairs was confirmed in dynamics calculation (software: Schrödinger MacroModel 9.5; duration 10^6 fs; 300 K) (Supplementary Figs. S11 and S12). For example, the inter-olefin distance in PEG6DMA in the presence of K^+ was in the range of 3.0 – 7.0 Å (>99 % probability) and 4.7 Å (d_{avg}) on average, while without K^+ the distance fluctuated more widely from 3.0 to 10 Å or beyond (>10 Å in ~50 % probability; d_{avg} = 8.7 Å). Similar simulation results were obtained for PEG5DMA and PEG8DMA. Additionally, d_{avg} for PEG6DMA decreased as a function of cations: template free (8.7 Å) > Cs^+ (7.9 Å) > Na^+ (5.2 Å) > K^+ (4.7 Å). Note that the CE in cyclopolymerization increased in the opposite order, demonstrating that the shorter d_{avg}. is, the more favored cyclopropagation.

Properties. Owing to some steric requirement upon cyclopropagation and/or the resulting cyclic repeat units, PPEGnDMAs exhibited stereoregularity different from the linear pendant counterparts (PPEG*n*MA).[18] Analyzed by ^{1}H and ^{13}C NMR (Table 1, Supplementary Fig. S7), PPEGnDMAs (n = 5, 6, 8) were more heterotactic than PPEG*n*MA (*n = 4*, *8.5*) [*mm*/*mr*/*rr* = 2.2/35.6/62.2 (PEG5DMA), 2.5/41.0/56.4 (PEG6DMA), 2.9/36.6/60.5 (PEG8DMA), 2.1/30.9/67.0 (PEG*4*MA), 1.9/29.9/68.2 (PEG*8.5*MA)]. While the stereoregularity for PPEG*n*MA was independent of the pendant length, that for PPEGnDMAs was dependent on the ring size (n).

Cyclopolymerization expectedly reduced the thermal mobility of the spacer PEG units. Determined by ^{13}C NMR, spin-lattice relaxation time (T_1) of the PEG spacer carbons in PPEG6DMA was 0.51 s, much shorter than those for the monomer (1.93 s) and for the linear pendants in PPEG*8.5*MA (1.68 s) (Supplementary Table S4). Within the cyclopolymers PPEGnDMA, T_1 decreased with decreasing the number of oxyethylene units (n): T_1 (n) = 0.48 (5), 0.51 (6), 0.68 (8); the shorter the spacer (the smaller ring size), the more limited the thermal mobility. The lowered mobility also supports the formation of cyclopolymers with "in-chain" polyether rings.

Because of the hydrophilic and thermosensitive PEG units, cyclopolymers of PEG6DMA and PEG8DMA were soluble in water at room temperature but underwent reversible, hysteresis-free phase transition in a narrow temperature range where lower critical solution temperature (LCST) was 35 and 50 ^oC, respectively (Supplementary Fig. S13). The LCST for PPEG6DMA was between those for non-cyclic counterparts from PEG2MA (~26 ^oC) and PEG3MA (~52 ^oC).[45,46] PPEG6DMA might provide attractive thermosensitive amphiphilic biomaterials with LCST close to human-body temperature.

Ion recognition. Given their consecutively placed in-chain crown ether units, recognition of metal cations was examined for PPEGnDMAs obtained with K^+ template (Fig. 4, Supplementary Figs. S14-S19, Supplementary Table S5). Thus, interaction of PPEG6DMA (DP = 12.5; M_n = 7900) with alkali metal salts (LiI, NaI, KI, KPF_6, and RbI; separately mixed with the polymer) was followed by ^1H NMR spectroscopy in an acetone-d_6/cyclohexanone mixed solvents (1/1, v/v) at 30 ^oC (Fig. 4a). Exposure to their cations induced downfield shifts in the PEG protons, indicative of cation encapsulation into the cyclic backbone cavity. The symmetrical Job plots peaked at $\chi = 0.5$ (molar fraction of the ring unit) demonstrated a 1:1 stoichiometeric interaction between a cation guest and an in-chain ring host. The cyclopolymer exhibited a stronger cation affinity than its monomer, judged from the association constant by ^1H NMR [K_a (M^{-1}): ~130 vs. ~70 with KPF_6; ~30 vs. ~0 (no interaction) with LiI]. Equally important, K^+ fitted to the cyclopolymer more efficiently than Li^+ [K_a (M^{-1}): ~130 (K^+) vs. ~30 (Li^+)] owing to the ring size suitable for K^+. The 1:1 cation binding also occurred in a MMA/PEG6DMA random copolymer (75/13 ratio in DP) consisting of the same cycloPEG units and the K_a (~140 M^{-1}) was similar to that with a PEG6DMA homopolymer. This indicates that each in-chain ring captures K^+ independently without interfering effects with neighboring units. The thermal mobility (T_1) of cycloPEG units decreased upon K^+ recognition (Supplementary Table S4).

However, the K^+ recognition by PPEGnDMA was dependent on the ring size (n) (Fig. 4b). The stoichiometry (K^+:cycloPEG unit) changed from 1:1 to 1:2 as n decreased from 6 to 4, judged

from the fact that the Job-plot maximum shifted from χ = 0.5 to 0.66. PPEG8DMA with larger in-chain rings captured K^+ in 1:1 stoichiometry four times more efficiently than PPEG6DMA [K_a (M^{-1}) = ~460 (PPEG8DMA), ~130 (PPEG6DMA)], though the 30-membered ring from PEG8DMA seemed too large for K^+ at first glance. Uniquely, the binding with PPEG8DMA preferentially occurred via the middle oxyethylene units [*d*: -(C$\underline{H_2}$C$\underline{H_2}$O)$_n$-] rather than via those adjacent to the ester linkages (*c*: -COOC$\underline{H_2}$CH$_2$O-), since the K_a for *d* is larger than the K_a for *c* [K_a (M^{-1}) = ~110 (*c*) vs. ~460 (*d*)]. This is because the 30-membered ring is spacious and flexible enough to mobilize some of the middle ether units, assuming a conformation better fit for the cation. In contrast, PPEG6DMA with rigid 24-membered rings apparently needs all the ring units [both middle (*d*) and ester-bound (*c*)] to capture K^+, as indicated by virtually no difference among their binding constants. The association constant of PPEGnDMA to K^+ [maximum: K_a (M^{-1}) = ~460] was smaller than that of crown ether derivatives with similar ring size under identical conditions (i.e. dibenzo-21-crown-7-ether to K^+: K_a (M^{-1}) = ~2.0 x 10^4) probably owing to strained conformation of the in-chain cyclized PEG units.

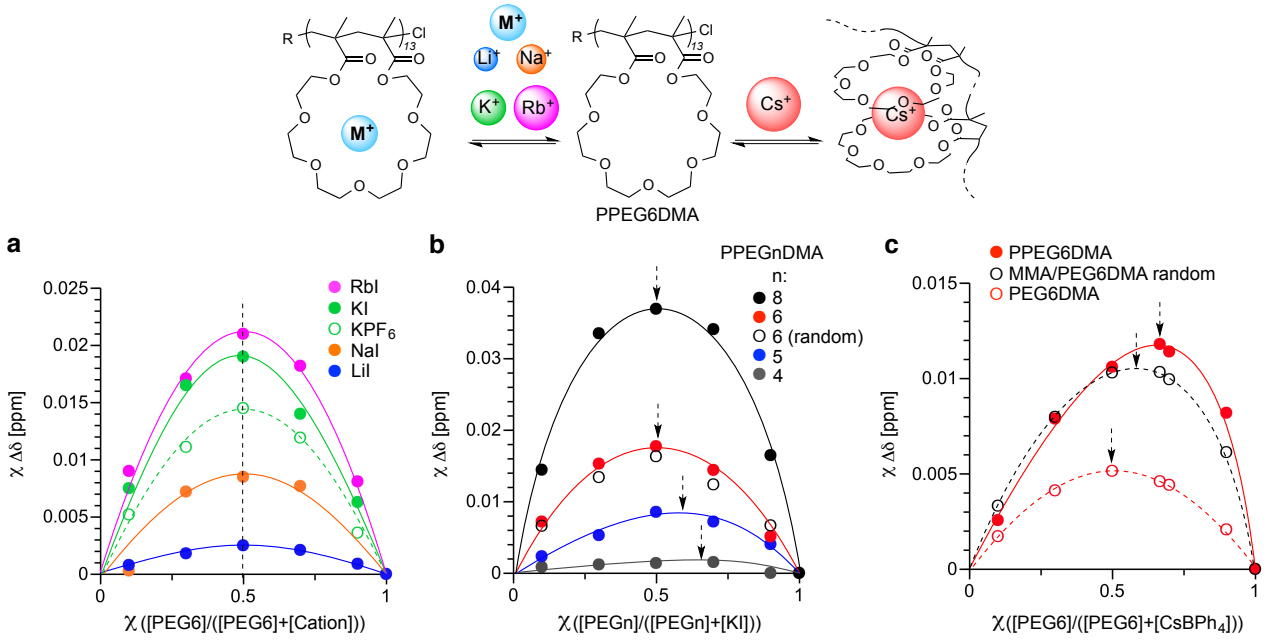

Figure 4: Cation recognition with poly(poly(ethylene glycol) dimethacrylate) (PPEGnDMA). Job plots for PPEGnDMA (n = 4-8) interacting with metal cations were based on ^{1}H NMR measurements of PPEGnDMA with metal cations in acetone-d_6/cyclohexanone (1/1) at 30 ^{o}C ([cyclicPEG units on PPEGDMA]$_0$ + [cation]$_0$ = 10 mM). (**a**) Job plots for PPEG6DMA with various metal cations (LiI, NaI, KPF_6, KI, RbI) support 1:1 recognition of their cations per a cycloPEG unit. (**b**) Effects of spacer length (n) of PPEGnDMA (homopolymer: filled circles; a MMA/PEG6DMA (75/13) random copolymer: open circle) on KI recognition (dash arrow: peak top). (**c**) $CsBPh_4$ recognition with PPEG6DMA (filled red circle), a MMA/PEG6DMA (75/13) random copolymer (open black circle), PEG6DMA (open red circle) (dash arrow: peak top). PPEGnDMA efficiently recognized a Cs^+ per two neighboring cyclicPEG units due to the local high density.

Recognition of a cesium cation ($CsBPh_4$) was further examined with cycloPEG homopolymers (PPEG6DMA, PPEG8DMA), a MMA/PEG6DMA (75/13) random copolymer, and their monomers (Fig. 4c, Supplementary Fig. S18). Their homopolymers bound one Cs^+ with two cycloPEG units (peak maximum in Job Plots: $\chi = 0.66$), whereas their monomers did Cs^+ via 1:1 stoichiometry (Cs^+: cycloPEG) as well as the other cations (Na^+, K^+, Rb^+: Supplementary Figs. S1). Such specific 1:2 recognition (Cs^+:cycloPEG) was independent of counter anion and solvents (CsI: recognized with two cycloPEG in CD_3OD). In contrast, the random copolymer competitively involved both 1:1 recognition and 1:2 counterpart (Cs^+:cycloPEG), where the peak maximum of the Job plot was at ~0.6 between 0.66 and 0.5. 18-Crown-6 in turn selectively showed 1:1 recognition. Thus, the unique 1:2 recognition for Cs^+ is attributed to the local high concentration of cycloPEG units per a chain. Confirmed by dynamic light scattering, PPEG6DMA in the presence of K^+ or Cs^+ had hydrodynamic radius (R_h) almost identical to PPEG6DMA alone [R_h = 6.3 nm (K^+ or Cs^+), 7.9 nm (non cation) in acetone], indicating that cycloPEG polymers intramolecularly grasped Cs^+ with the two neighbour cycloPEG units within a single chain.

Selective/competitive ion recognition. The efficiency and selectivity in the cation recognition by PPEG6DMA was further evaluated in competitive recognition. Thus, in cyclohexanone/acetone-d_6 (1/1, v/v), the polymer was mixed with an equimolar mixture of Na and another alkali metal cation, and the selectivity was evaluated in monitoring the sodium guest by ^{23}Na NMR spectroscopy (Fig. 5); obviously, ^1H or ^{13}C NMR is totally useless in this analysis, because there was little difference in chemical shift between cyclic PEG units with Na and with another cation. This method will also provide evidence for recognition not from the host (PEG by NMR) but from the guest (cation).

In the presence of PPEG6DMA, the Na signal of NaI shifted to upfield by $\Delta\delta = -1.53$ ppm and broadened [half width: 350 Hz from 19.8 Hz (polymer-free salt)]. The peak shift and broadening was larger than with the monomer (–0.96 ppm and 40 Hz) and with PPEG3MA (a linear pendant counterpart to PPEG6DMA: –0.34 ppm and 135 Hz), again demonstrating the efficient cation binding by ^{23}Na NMR.

More importantly, PPEG6DMA selectively recognized Na^+ over Li^+ or Bu_4N^+ and in turn did K^+ over Na^+ in competitive experiments where an equimolar mixture of the probe and another cation was exposed to the cyclopolymer. The upfield shift and broadening for the sodium signal of NaI with PPEG6DMA were still maintained in the presence of Bu_4NI and LiI. However, KI made the sodium signal shifting to downfield (close to original position) again and narrow. This implies that the presence of competing cations does not seriously interfere the recognition of a preferred cation and that the cation selectivity in PPEG6DMA increases in the order $Bu_4N < Li <$

Na < K. In addition, in-chain cyclic PEG units are essential for the selective recognition, since PPEG3MA turned out poorly selective in cation recognition (Supplementary Fig S19).

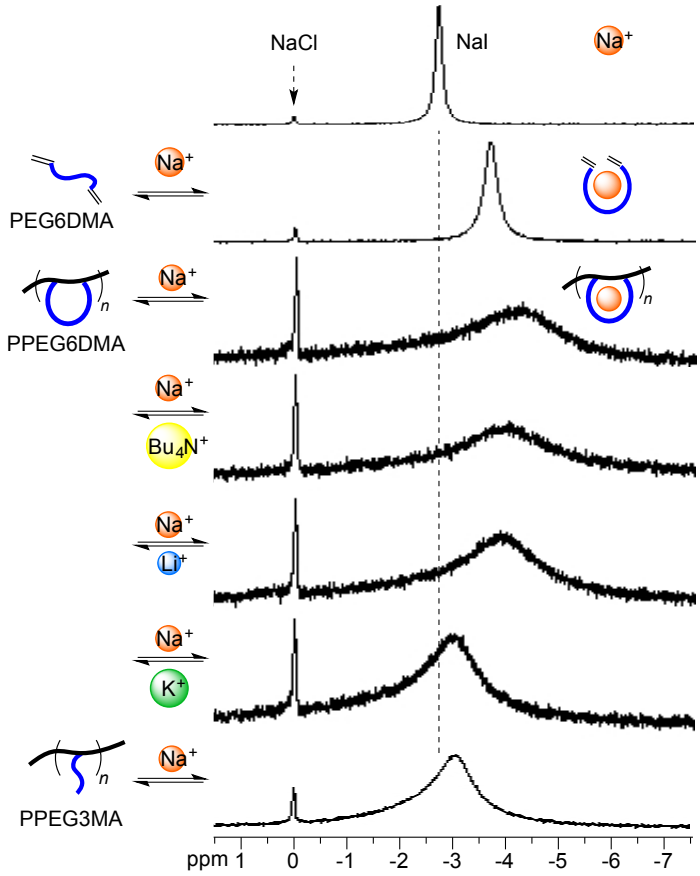

Figure 5: Competitive cation recognition with poly(hexaethylene glycol dimethacrylate) (PPEG6DMA). ^{23}Na NMR measurements of NaI with PPEG6DMA in the presence of other cations (Bu_4NI, LiI, KI) were conducted in acetone-d_6/cyclohexanone (1/1, v/v) at 30 ^{o}C. Owing to the "in-chain" cyclic PEG structure, PPEG6DMA recognized NaI more efficiently than PEG6DMA (monomer) and poly(triethylene glycol methyl ether methacrylate) (PPEG3MA: linear pendant). Additionally, PPEG6DMA performed Na^+ recognition selective over Bu_4N^+ or Li^+, and K^+ recognition over Na^+.

Discussion

Cyclopolymerization of divinyl monomers for linear polymers containing in-chain cyclic structures essentially undergoes alternating propagation process of intramolecular cyclization and intermolecular addition, in which the efficient intramolecular cyclization is a key step to prevent the intermolecular crosslinking of polymer chains. In cation template-assisted cyclopolymerization, a potassium cation (K^+) effectively interacts with PEG-bearing dimethacrylates, PEGnDMA (n = 5-8) to transform the random conformation into the pseudo-cyclized counterpart. As a result, the two vinyl groups come close to be suitable for intramolecular cyclization. Owing to high tolerance to polar functional groups including metal cations,[19,20] a ruthenium catalytic system efficiently induce controlled radical cyclopolymerization of PEGnDMA in the presence of a potassium cation to directly give linear polymers (PPEGnDMA) bearing large (19-30 membered) in-chain cyclic PEG rings with controlled molecular weight.

The resulting PPEGnDMAs further work as unique nano cavities to recognize metal cations, more efficiently and selectively than linear pendant counterparts and an original monomer. In the present design, the binding constant to metal cations is smaller than that with corresponding crown ethers. This is probably because cyclized PEG rings in PPEGnDMAs have steric strain and/or irregular conformation originating from the ill-controlled stereoregularity, though PPEGnDMAs (n = 5-8) obtained with a potassium template are more heterotactic than linear counterparts (PPEGMAs). Thus, development of stereoregular cyclopolymerization of PEGnDMA would be important to improve that issue; such polymerization system could produce cycloPEG polymers with highly regulated ring conformation to induce cooperative recognition of cationic compounds more efficiently and selectively than conventional crown ethers. In addition, cation template-assisted polymerization is quite versatile to afford various primary structures from simple cyclopolymers to random and block copolymers containing cyclized PEGnDMA units. In the future, cycloPEG-bearing microgel star polymers might be useful as efficient and selective scavengers to extract (or remove) metal cations from solution, because microgel star polymers potentially behave as nanocapsules to capture molecules and can be easily recovered from solution by modulating the arm species.[41]

In conclusion, we have successfully developed cation template-mediated, controlled radical cyclopolymerization of PEG spacer-bearing dimethacrylates, PEGnDMA (n = 4-8) for polymeric pseudo crown ethers performing unique cation recognition. The synergistic marriage of supramolecular chemistry and polymer chemistry opens a new efficient strategy to create well-defined functional cyclopolymers from common reagents with simple templates. Multi-control of primary structures and/or tailor-made design of three-dimensional architectures

would further advance cycloPEG-based polymers as novel functional macromolecules to innovate on molecular recognition.

Methods

Materials. Triethylene glycol monomethyl ether (Aldrich, purity >95%), tetraethylene glycol (TCI, purity >95%), pentaethylene glycol (TCI, purity > 95%), hexaethylene glycol (Aldrich, purity >97%), octaethylene glycol (Wako, purity >97%), tetrahydrofuran (THF: Wako; dehydrated), diethyl ether (Wako, purity >99.5%), sodium sulfate (Wako, purity >99%), and 25% ammonia solution (Wako) were used as received. Methacryloyl chloride (TCI, purity >80%) and triethylamine (TCI, purity >99%) were purified by distillation before use.

Methyl methacrylate (MMA: TCI; purity >99%) was dried overnight over calcium chloride and purified by double distillation under reduced pressure from calcium hydride before use. Poly(ethylene glycol) dimethacrylate (PEGnDMA: n = [-(CH_2CH_2O)-]/[PEGnDMA] = 4, 5, 6, 8) was synthesized as shown below. Triethylene glycol methyl ether methacrylate (PEG3MA) was prepared according to the literature.[45] Poly(ethylene glycol) methyl ether methacrylate [PEG*n*MA: M_n = 475 (*n = 8.5*); M_n = 300 (*n = 4*); Aldrich] was purified by an inhibitor remover column (Product No.: 311332, Aldrich) and was degassed by vacuum-argon purge cycles before use. Ethyl α-chlorophenylacetate (ECPA: Aldrich; purity >97%) was purified by distillation under reduced pressure before use. H-$(MMA)_2$-Cl was prepared according to the literature.[44] $RuCp^*Cl(PPh_3)_2$ (Cp^*: pentamethylcyclopentadienyl, Aldrich, purity >97%) was used as received and was handled in a grove box under a moisture- and oxygen-free argon atmosphere (H_2O < 1 ppm, O_2 < 1 ppm). *n*-Bu_3N (TCI, purity > 98%) was degassed by vacuum-argon purge cycles before use. Tetralin (1,2,3,4-tetrahydronaphthalene) (Kisida Chemical, purity >98%)], as an internal standard to check the conversion of PEGn(D)MA by ^1H nuclear magnetic resonance (NMR), was dried over calcium chloride overnight and distilled twice from calcium hydride. Cyclohexanone (Wako, purity >99%) was dried on molecular sieves 4A (Wako) and degassed by vacuum-argon purge cycles before use. Methanol (Wako, purity > 99.8%) and regenerated cellulose dialysis membranes (Spectra/Por® 7; MWCO 1000) for polymer purification were used as received.

Lithium iodide (LiI: Aldrich; purity >99%), sodium iodide (NaI: Aldrich; purity >99.9%), potassium iodide (KI: Wako; purity >99%), potassium hexafluorophosphate (KPF_6: Aldrich; purity >98%), rubidium iodide (RbI: Aldrich; purity >99.9%), cesium iodide (CsI: Aldrich; purity >99.9%), cesium tetraphenylborate ($CsBPh_4$: Aldrich; purity >98%), 18-crown-6 (Wako, purity >98%), dibenzo-21-crown-7-ether (TCI, purity >96%), and acetone-d_6 (CIL) were used as received.

Monomer Synthesis. A typical procedure for PEG6DMA was given: In 200 mL round-bottomed flask filled with argon, methacryloyl chloride (94.6 mmol, 9.1 mL) was added dropwise to a solution of hexaethylene glycol (31.5 mmol, 10 mL) and triethylamine (94.6 mmol, 6.3 mL) in dry THF (70 mL) at 0 ^{o}C. The reaction mixture was stirred at 0 ^{o}C for 2 h and at 25 ^{o}C for an additional 22 h, and then evaporated under reduced pressure. The concentrated crude was diluted with diethyl ether (150 mL) and washed with water (150 mL). The aqueous layer was separated and further extracted with diethyl ether (150 mL). The combined ether solution was washed with 200 mL of 25% ammonia water three times and with 200 mL of distilled water once, and was dried on sodium sulfate overnight. Into the purified ether solution of PEG6DMA, dried cyclohexanone was added. The solution was then evaporated under reduced pressure to remove the ether to give cyclohexanone solution of PEG6DMA for cyclopolymerization. ^{1}H NMR [500 MHz, acetone-d_6, r.t., δ = 2.05 ppm (acetone)]: δ 6.08 (m, olefin, 2H), 5.62 (m, olefin, 2H), 4.24 (t, J = 4.8 Hz, 4H, -COOCH_2CH$_2$O-), 3.71 (t, J = 4.8 Hz, 4H, -COOCH$_2$CH_2O-), 3.62-3.56 (m, 16H, -OCH_2CH_2O-), 1.92 (m, 6H, -CCH_3). ^{13}C NMR [125 MHz, acetone-d_6, r.t., δ = 206.5 ppm (acetone)]: δ 168.0, 138.0, 126.3, 72.0, 70.3, 65.3, 19.2. ESI-MS m/z ([M + Na]$^{+}$): calcd. for $C_{20}H_{34}O_9Na$ 441.2, found 441.2.

Polymerization. Cation template-assisted living radical cyclopolymerization of PEGnDMA (n = 4-8) was carried out by the syringe technique under argon in baked glass tubes equipped with a three-way stopcock. PEGnDMA was pre-mixed with KPF_6 in cyclohexanone at predetermined ratio ([PEGnDMA]/[KPF_6] = 1/1-1/5) to give a cyclohexanone solution of PEG6DMA interacting with KPF_6. A typical procedure for PPEG6DMA (DP = 12.5) was given: RuCp*Cl(PPh_3)$_2$ (0.005 mmol, 4.0 mg) was placed in a 30 mL glass tube. Into the tube, cyclohexanone (8.7 mL), tetralin (0.1 mL), a 400 mM toluene solution of n-Bu_3N (0.2 mmol, 0.5 mL), a 789 mM cyclohexanone solution of PEG6DMA with KPF_6 ([PEG6DMA] = 0.25 mmol, [KPF_6] = 0.5 mmol, 0.32 mL), and a 57.6 mM toluene solution of H-(MMA)$_2$-Cl (0.02 mmol, 0.35 mL) were added sequentially in this order at 25 ^{o}C under argon. The tube containing the mixture (total volume: 10 mL) was placed in an oil bath at 40 ^{o}C. In predetermined intervals, a small portion of the reaction mixture was sampled and cooled to -78 ^{o}C to terminate the reaction. The conversion of PEG6DMA was then determined by ^{1}H NMR measurement with an internal standard (tetralin) in $CDCl_3$ at r.t.. After 56h (conversion = 87%), the quenched reaction mixture was evaporated to dryness under reduced pressure. The resulting crude was first fractionated by preparative SEC in DMF and then dialyzed in water with a regenerated cellulose membrane (Spectra/Por® 7; MWCO 1000) for 5 day. The inner solution was evaporated to dryness under reduced pressure to give PPEG6DMA. SEC (DMF, 0.01 M LiBr): M_n = 7900 g/mol; M_w/M_n = 1.20. ^{1}H NMR [500 MHz, $CDCl_3$, δ = 7.26

($CHCl_3$)]: δ 6.2, 5.6 (olefin), 4.2-4.0 (-COOC*H*$_2$CH$_2$O-), 3.8-3.5 (-OC*H*$_2$C*H*$_2$O-), 2.1-1.3 (-C*H*$_2$CCH$_3$), 1.3-0.8 (-CC*H*$_3$). CE = ~99%. ^{13}C NMR [125 MHz, $CDCl_3$, δ = 77.0 ($CHCl_3$)]: δ 178.2-175.5 (C=O), 71.1-70.2 (-O*C*H$_2$*C*H$_2$O-), 68.8-68.4 (-COOCH$_2$*C*H$_2$O-), 64.6-63.8 (-COO*C*H$_2$CH$_2$O-), 55.5-52.0 (-CH$_2$*C*(CH$_3$)CO-), 45.6-44.5 (-*C*H$_2$C(CH$_3$)CO-), 22.6-16.0 (-*C*H$_3$). *mm*/*mr*/*rr* = 2.5/41.0/56.4.

Characterization. The MWD, M_n, and M_w/M_n ratios of polymers were measured by size-exclusion chromatography (SEC) in DMF containing 10 mM LiBr at 40 °C (flow rate: 1 mL/min) on three linear-type polystyrene gel columns (Shodex KF-805L; exclusion limit = 4×10^6; particle size = 10 μm; pore size = 5000 Å; 0.8 cm i.d. × 30 cm) that were connected to a Jasco PU-2080 precision pump, a Jasco RI-2031 refractive index detector, and a Jasco UV-2075 UV/vis detector set at 270 nm. The columns were calibrated against ten standard poly(MMA) samples (Polymer Laboratories; M_n = 1000–1200000; M_w/M_n = 1.06–1.22). Polymer samples to analyze the structure and investigate the cation recognition were fractionated by preparative SEC (column: Shodex K-2003; exclusion limit = 7×10^4; particle size = 6 μm; pore size = 500 Å; 2.0 cm i.d. × 30 cm, eluent: DMF) and dialyzed with regenerated cellulose membranes in methanol.

^{1}H, ^{13}C, and ^{23}Na nuclear magnetic resonance (NMR) spectra were recorded in acetone-d_6, DMSO-d_6, and $CDCl_2$ at 30 °C on a JEOL JNM-LA500 spectrometer, operating at 500 (^{1}H), 125 (^{13}C), and 132 (^{23}Na) MHz, respectively. Matrix-assisted laser desorption/ionization time of flight mass spectrometry (MALDI-TOF-MS) analysis was performed on a Shimadzu AXIMA-CFR instrument equipped with 1.2 m linear flight tubes and a 337 nm nitrogen laser with dithranol (1,8,9-anthracenetriol) as an ionizing matrix and sodium trifluoroacetate as a cationizing agent. Electorospray ionization mass spectrometry (ESI-MS) was performed on Waters Quattro micro API. Dynamic light scattering (DLS) was measured on Otsuka Photal ELSZ-0 equipped with a semi-conductor laser (wavelength: 658 nm) at 25 °C. The measuring angle was 165°, and the data was analyzed by CONTIN fitting method.

Ultraviolet-visible (UV/Vis) spectra were obtained from Shimadzu UV-1800 in H_2O or CH_2ClCH_2Cl at room temperature (optical path length = 1.0 cm). The cloud points of polymers in water were determined by the transmittance of aqueous solution of polymers and monitored at 660 nm by changing the solution temperature between 20 °C and 80 °C (optical path length = 1.0 cm; heating rate: 1 °C/min; cooling rate: -1 °C/min) on Shimadzu UV-1800.

References

1. Meeuwissen, J. & Reek, J. N. H. Supramolecular catalysis beyond enzyme mimics. *Nature Chem.* **2**, 615-621 (2010).
2. Suzuki, K., Sato, S. & Fujita, M. Template synthesis of precisely monodisperse silica nanoparticles within self-assembled organometallic spheres. *Nature Chem.* **2**, 25-29 (2010).
3. McHale, R., Patterson, J. P., Zetterlund, P. B. & O'Reilly, R. K. Biomimetic radical polymerization via cooperative assembly of segregating templates. *Nature Chem.* **4**, 491-497 (2012).
4. Pedersen, C. J. Cyclic polyethers and their complexes with metal salts. *J. Am. Chem. Soc.* **89**, 7017-7036 (1967).
5. Meyer, C. D., Joiner, C. S. & Stoddart, J. F. Template-directed synthesis employing reversible imine bond formation. *Chem. Soc. Rev.* **36**, 1705-1723 (2007).
6. Crowley, J. D., Goldup, S. M., Lee, A.-L., Leigh, D. A. & McBurney, R. T. Active metal template synthesis of rotaxanes, catenanes and molecular shuttles. *Chem. Soc. Rev.* **38**, 1530-1541 (2009).
7. Zhang, M., Zhu, K. & Huang, F. Improved complexation of paraquat derivatives by the formation of crown ether-based cryptands. *Chem. Commun.* **46**, 8131-8141 (2010).
8. Marsella, M. J., Maynard, H. D. & Grubbs, R. H. Template-directed ring-closing metathesis: synthesis and polymerization of unsaturated crown ether analogs. *Angew. Chem. Int. Ed.* **36**, 1101-1103 (1997).
9. Cantrill, S. J., Grubbs, R. H., Lanari, D., Leung, K. C.-F., Nelson, A., Poulin-Kerstien, K. G., Smidt, S. P., Stoddart, J. F. & Tirrell, D, A. Template-directed olefin cross metathesis. *Org. Lett.* **7**, 4213-4216 (2005).
10. Belowich, M. E., Valente, C., Smaldone, R. A., Friedman, D. C., Thiel, J., Cronin, L. & Stoddart, J. F. Positive cooperativity in the template-directed synthesis of monodisperse macromolecules. *J. Am. Chem. Soc.* **134**, 5243-5261 (2012).
11. Tan, Y. Y. The synthesis of polymers by template polymerization. *Prog. Polym. Sci.* **19**, 561-588 (1994).
12. Połowinski, S. Template polymerization and co-polymerization. *Prog. Polym. Sci.* **27**, 537-577 (2002).
13. Serizawa, T., Hamada, K. & Akashi, M. Polymerization within a molecular-scale stereoregular template. *Nature* **429**, 52-55 (2004).
14. South, C. R. & Weck, M. Template-enhanced ring-opening metathesis polymerization. *Macromolecules* **40**, 1386-1394 (2007).
15. Wan, D., Satoh, K. & Kamigaito, M. Triple hydrogen bonding for stereospecific radical

polymerization of a DAD monomer and simultaneous control of tacticity and molecular weight. *Macromolecules* **39**, 6882-6886 (2006).

16. Ida, S., Terashima, T., Ouchi, M. & Sawamoto, M. Selective radical addition with a designed heterobifunctional halide: a primary study toward sequence-controlled polymerization upon template effect. *J. Am. Chem. Soc.* **131**, 10808-10809 (2009).
17. Ida, S., Ouchi, M. & Sawamoto, M. Designer template initiator for sequence regulated polymerization: system design for substrate-selective metal-catalyzed radical addition and living radical polymerization. *Macromol. Rapid. Commun.* **32**, 209-214 (2009).
18. Hibi, Y., Tokuoka, S., Terashima, T., Ouchi, M. & Sawamoto, M. Design of AB divinyl "template monomers" toward alternating sequence control in metal-catalyzed living radical polymerization. *Polym. Chem.* **2**, 341-347 (2011).
19. Ouchi, M., Terashima, T. & Sawamoto, M. Precision control of radical polymerization via transition metal catalysis: from dormant species to designed catalysts for precision functional polymers. *Acc. Chem. Res.* **41**, 1120-1132 (2008).
20. Ouchi, M., Terashima, T. & Sawamoto, M. Transition metal-catalyzed living radical polymerization: toward perfection in catalysis and precision polymer synthesis. *Chem. Rev.* **109**, 4963-5050 (2009).
21. Tsarevsky, N. V. & Matyjaszewski, K. "Green" atom transfer radical polymerization: from process design to preparation of well-defined environmentally friendly polymeric materials. *Chem. Rev.* **107**, 2270-2299 (2007).
22. Matyjaszewski, K. & Tsarevsky, N. V. Nanostructured functional materials prepared by atom transfer radical polymerization. *Nature Chem.* **1**, 276-288 (2009).
23. Butler, G. B. Cyclopolymerization. *J. Polym. Sci. Part A: Polym. Chem.* **38**, 3451-3461 (2000).
24. Yokota, K., Haba, O., Satoh, T. & Kakuchi, T. Cyclopolymerization. Chirality induction for the synthesis of chiroselective corand/ionophore ligands. *Macromol. Chem. Phys.* **196**, 2383-2416 (1995).
25. Tunca, U. & Yagci,Y. Crown ether-containing polymers. *Prog. Polym. Sci.* **19**, 233-286 (1994).
26. Kodaira, T. Structural control during the cyclopolymerization of unconjugated dienes. *Prog. Polym. Sci.* **25**, 627-676 (2000).
27. Choi, S.-K., Gal, Y.-S., Jin, S.-H. & Kim, H.-K. Poly(1,6-heptadiyne)-based materials by metathesis polymerization. *Chem. Rev.* **100**, 1645-1681 (2000).
28. Jia, Y., Liu, L., Lei, B., Li, J. & Zhu, X. X. Crown ether cavity-containing copolymers via controlled alternating cyclopolymerization. *Macromolecules* **44**, 6311-6317 (2011).

29. Ochiai, B., Ootani, Y. & Endo, T. Controlled cyclopolymerization through quantitative 19-membered ring formation. *J. Am. Chem. Soc.* **130**, 10832-10833 (2008).
30. Narumi, A., Sakai, R., Ishido, S., Sone, M., Satoh, T., Kaga, H., Nakade, H. & Kakuchi, T. Enantiomer-selective radical polymerization of bis(4-vinylbenoate)s with chiral atom transfer radical polymerization initiating system. *Macromolecules* **40**, 9272-9278 (2007).
31. Nakano, T., Okamoto, Y., Sogah, D. Y. & Zheng, S. Cyclopolymerization of optically active (-)-trans-4,5-bis({methacryloyloxy}diphenylmethyl)-2,2-dimethyl-1,3-dioxacyclopentene through radical and anionic mechanisms given highly isotactic polymers. *Macromolecules* **28**, 8705-8706 (1995).
32. Kakuchi, T., Haba, O. & Yokota, K. Cyclopolymerization of divinyl ethers. Synthesis and the cation-binding property of poly(crown ether)s. *Macromolecules* **25**, 4854-4858 (1992).
33. Coates, G. W. & Waymouth, R. M. Enantioselective cyclopolymerization: optically active poly(methylene-1,3-cyclopentane). *J. Am. Chem. Soc.* **113**, 6270-6271 (1991).
34. Coates, G. W. & Waymouth, R. M. Enatioselective cyclopolymerization of 1,5-hexadiene catalyzed by chiral zirconocenes: A novel strategy for the synthesis of optically active polymers with chirality in the main chain. *J. Am. Chem. Soc.* **115**, 91-98 (1993).
35. Fox, H. H. & Schrock, R. R. Living cyclopolymerization of diethyl dipropargylmalonate by Mo(CH-*t*-Bu)(NAr)[OCMe$(CF_3)_2$]$_2$ in dimethoxyethane. *Organometallics* **11**, 2763-2765 (1992).
36. Kumar, P. S., Wurst, K. & Buchmeiser, M. R. Factors relevant for the regioselective cyclopolymerization of 1,6-heptadiynes, *N*,*N*-dipropargylamines, *N*,*N*-dipropargylammonium salts, and dipropargyl ethers by Ru^{IV}-alkylidene-based metathesis initiators. *J. Am. Chem. Soc.* **131**, 387-395 (2009).
37. Kopolow, S., Hogen Esch, T. E. & Smid, J. Poly(vinyl macrocyclic polyethers). Synthesis and cation binding properties. *Macromolecules* **6**, 133-142 (1973).
38. Warshawsky, A., Kalir, R., Deshe, A., Berkovitz, H. & Patchornik, A. Polymeric Pseudocrown ethers. 1. Synthesis and complexation with transition metal anions. *J. Am. Chem. Soc.* **101**, 4249-4258 (1979).
39. Alexandratos, S. D. & Stine, C. L. Synthesis of ion-selective polymer-supported crown ethers: A review. *React. Funct. Polym.* **60**, 3-16 (2004).
40. Gao, H. & Matyjaszewski, K. Synthesis of functional polymers with controlled architecture by CRP of monomers in the presence of cross-linkers: From stars to gels. *Prog. Polym. Sci.* **34**, 317-350 (2009).
41. Terashima, T. & Sawamoto, M. Microgel-Core Star Polymers as Functional Compartments for Catalysis and Molecular Recognition, in Matyjaszewski, K., Sumerlin, B. S. & Tsarevski, N. V.

eds. *Progress in Controlled Radical Polymerization: Materials and Applications*, ACS Symposium Series **1101**, 65-80 (2012).

42. Terashima, T., Nomura, A., Ito, M., Ouchi, M. & Sawamoto, M. Star-polymer-catalyzed living radical polymerization: Microgel-core reaction vessel by tandem catalyst interchange. *Angew. Chem. Int. Ed.* **50**, 7892-7895 (2011).
43. Baek, K.-Y., Kamigaito, M. & Sawamoto, M. Star-shaped polymers by metal-catalyzed living radical polymerization. 1. Design of Ru(II)-based systems and divinyl linking agents. *Macromolecules* **34**, 215-221 (2001).
44. Ando, T., Kamigaito, M. & Sawamoto, M. *Macromolecules* **31**, 6708-6711 (1998).
45. Han, S., Hagiwara, M. & Ishizone, T. *Macromolecules* **36**, 8312-8319 (2003).
46. Lutz, J.-F. Polymerization of oligo(ethylene glycol) (meth)acrylates: Toward new generations of smart biocompatible materials. *J. Polym. Sci. Part A: Polym. Chem.* **46**, 3459-3470 (2008).

Acknowledgements

This research was supported by the Ministry of Education, Science, Sports and Culture through a Grant-in-Aid for Creative Scientific Research (18GS0209) and Young Scientist (B) (No.20750091), and by the foundation for the promotion of ion engineering, for which T.T. is grateful. We also thank Prof. Kenji Matsuda and Prof. Takashi Hirose (Department of Synthetic Chemistry and Biological Chemistry, Kyoto University) for molecular dynamics calculation, and Mr. Yuta Koda for technical supports on ^{23}Na NMR measurements.

Author contributions

T.T. and M.K. designed all of experiments. M.K., Y.M., and H.Y. carried out the experiments. T.T. and M.S. conceived and supervised the project and wrote the paper.

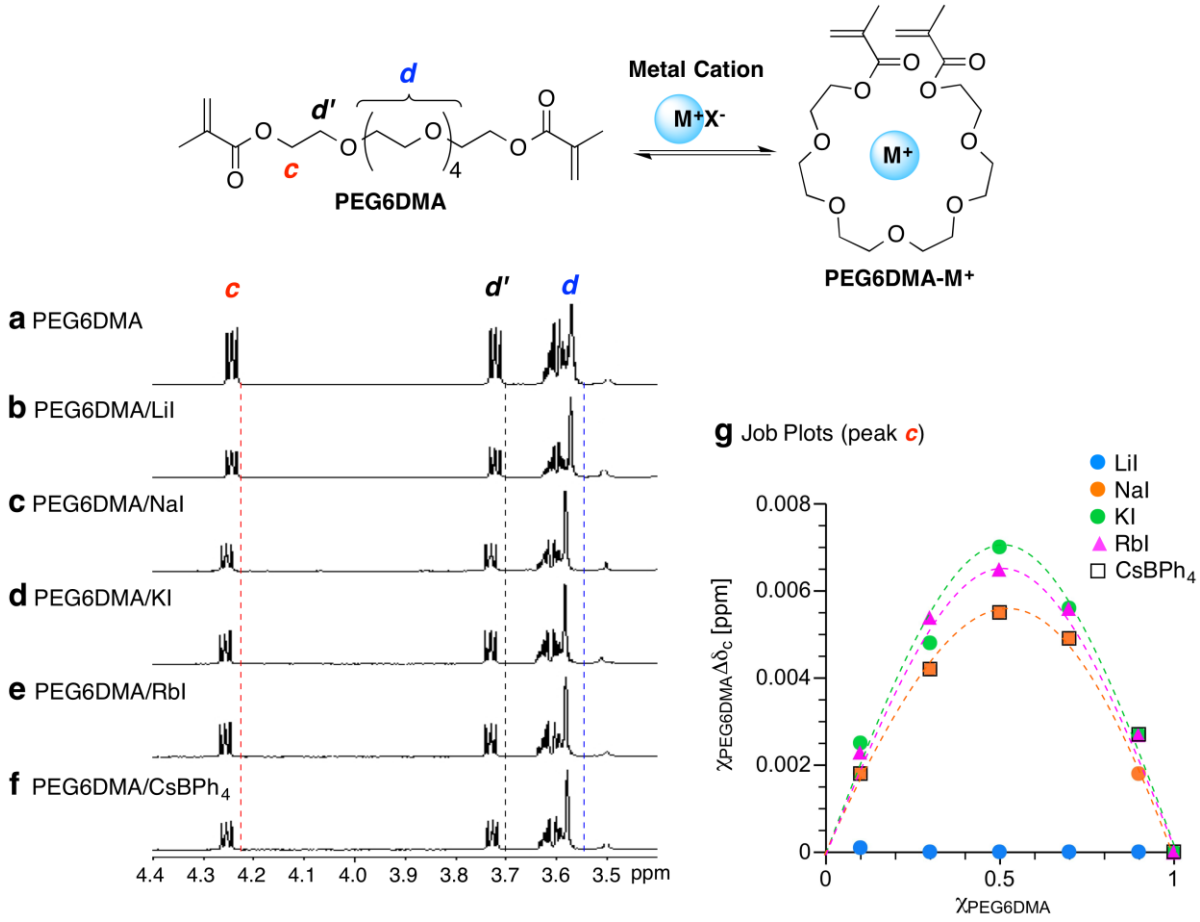

Supplementary Figure S1: Interaction of PEG6DMA with cation templates. ^{1}H NMR spectra of PEG6DMA in the presence of metal cations [M^+: none (**a**), LiI (**b**); NaI (**c**); KI (**d**); RbI (**e**); $CsBPh_4$ (**f**)]: [PEG6DMA]/[M^+] = 5/5 mM in acetone-d_6/cyclohexanone (1/1, v/v) at 30 ^{o}C. (**g**) Job plots for the association of PEG6DMA with metal cations (Li^+, Na^+, K^+, Rb^+, Cs^+) from the change in chemical shift (ppm) of the peak *c*: [PEG6DMA] + [M^+] = 10 mM in acetone-d_6/cyclohexanone at 30 ^{o}C; $\chi_{PEG6DMA}$: mole fraction of PEG6DMA. PEG6DMA formed a 1:1 complex with Na^+, K^+, Rb^+, and Cs^+, except for Li^+.

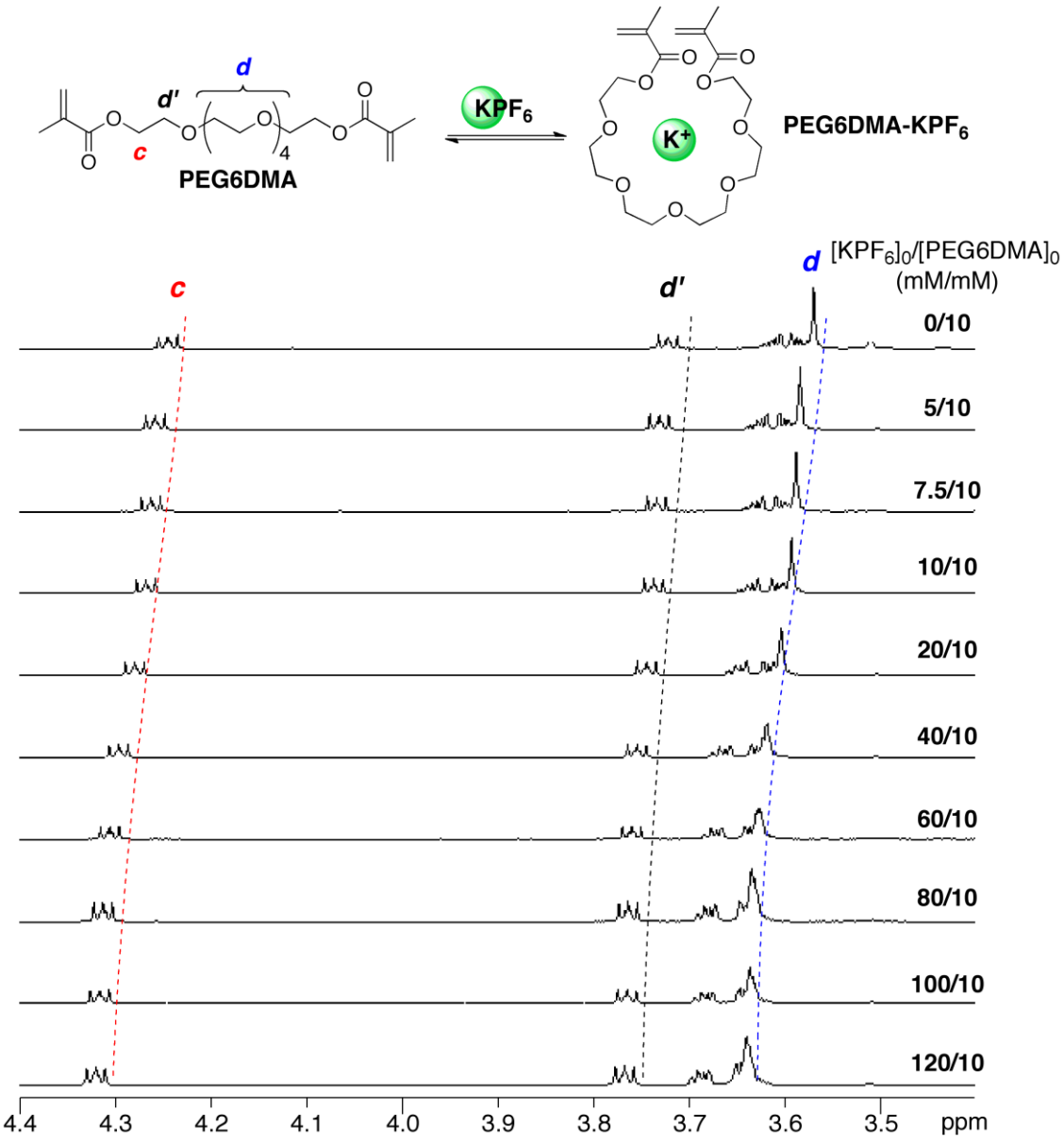

Supplementary Figure S2: ^{1}H NMR titration experiments of with KPF_6. Condition: $[PEG6DMA]_0/[KPF_6]_0$ = 10/0 – 120 mM in acetone-d_6/cyclohexanone (1/1, v/v) at 30 ^{o}C.

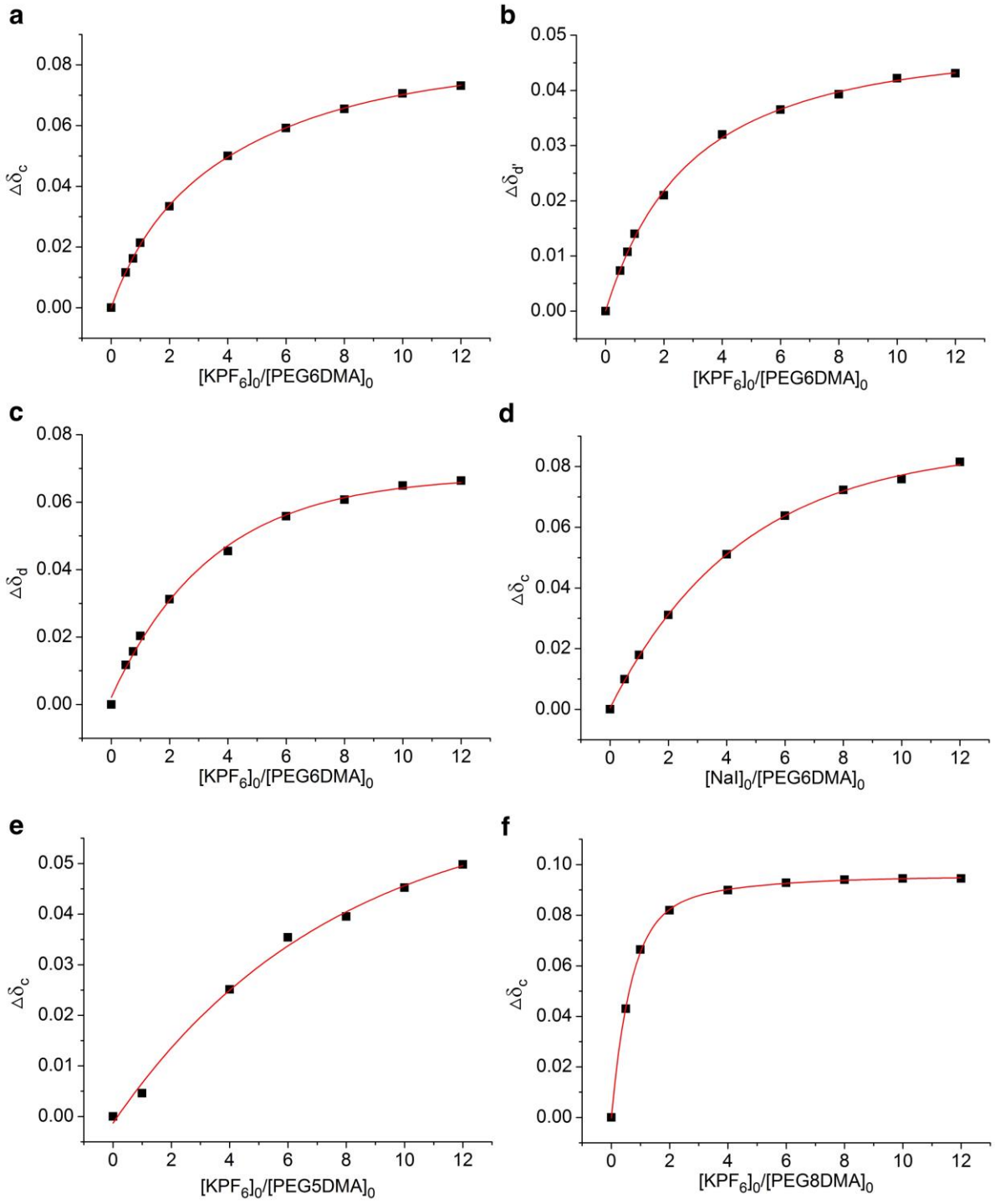

Supplementary Figure S3: Curve fitting for the chemical shift change of PEG protons of PEGnDMA with metal catios. Peaks *c*, *d'*, and *d*: assigned in Figure S2. $[PEGnDMA]_0$/[metal cations]$_0$ = 10/0-120 mM in acetone-d_6/cyclohexanone (1/1, v/v) at 30 ^oC. Peaks *c* (**a**), *d'* (**b**), and *d* (**c**) for PEG6DMA with KPF_6. (**d**) Peak *c* for PEG6DMA with NaI. Peaks *c* for PEG5DMA (**e**) or PEG8DMA (**f**) with KPF_6.

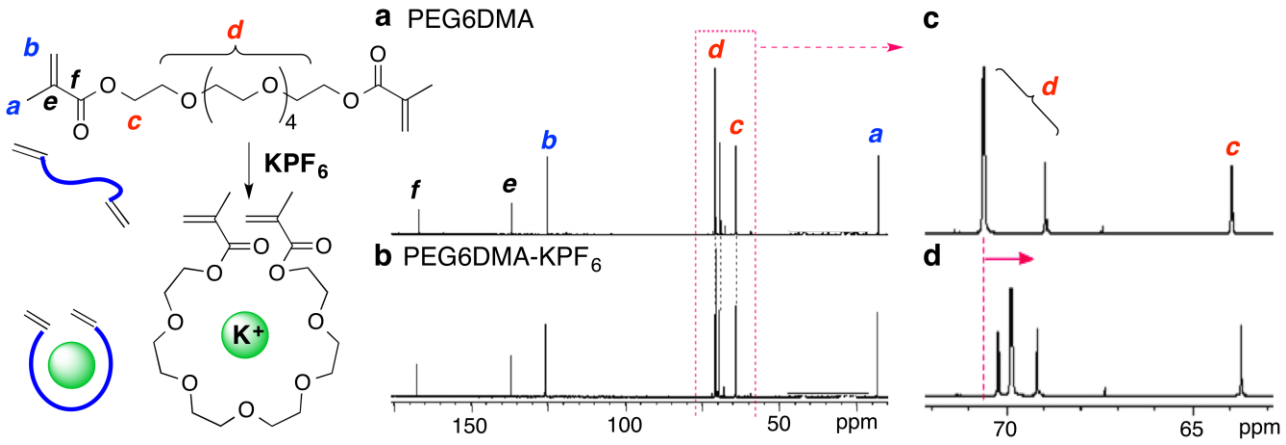

Supplementary Figure S4: ^{13}C NMR spectra of PEG6DMA with KPF_6. [PEG6DMA]/[KPF_6] = 120/0 (**a**,**c**) or 240 (**b**,**d**) mM in acetone-d_6/cyclohexanone (1/1, v/v) at 30 ^{o}C.

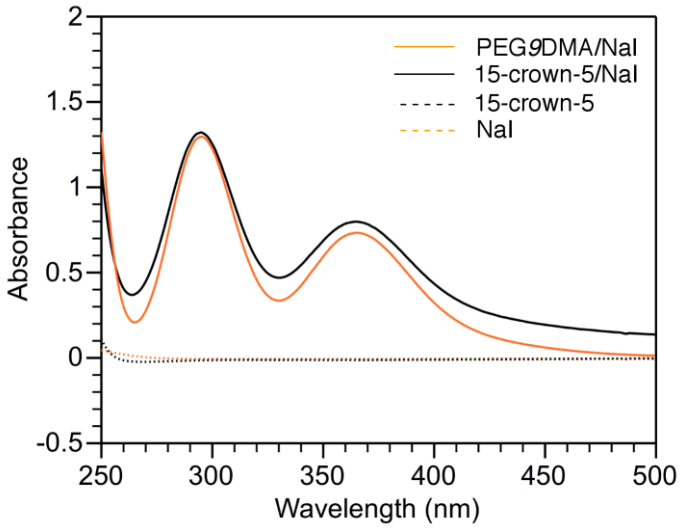

Supplementary Figure S5: UV-vis spectra of NaI with PEG*9*DMA or 15-crown-5. PEG*9*DMA/NaI (0.2 mM), 15-crown-5/NaI (0.5 mM), and 15-crown-5 (0.5 mM) in CH_2ClCH_2Cl and NaI (0.2 mM) in H_2O at r.t..

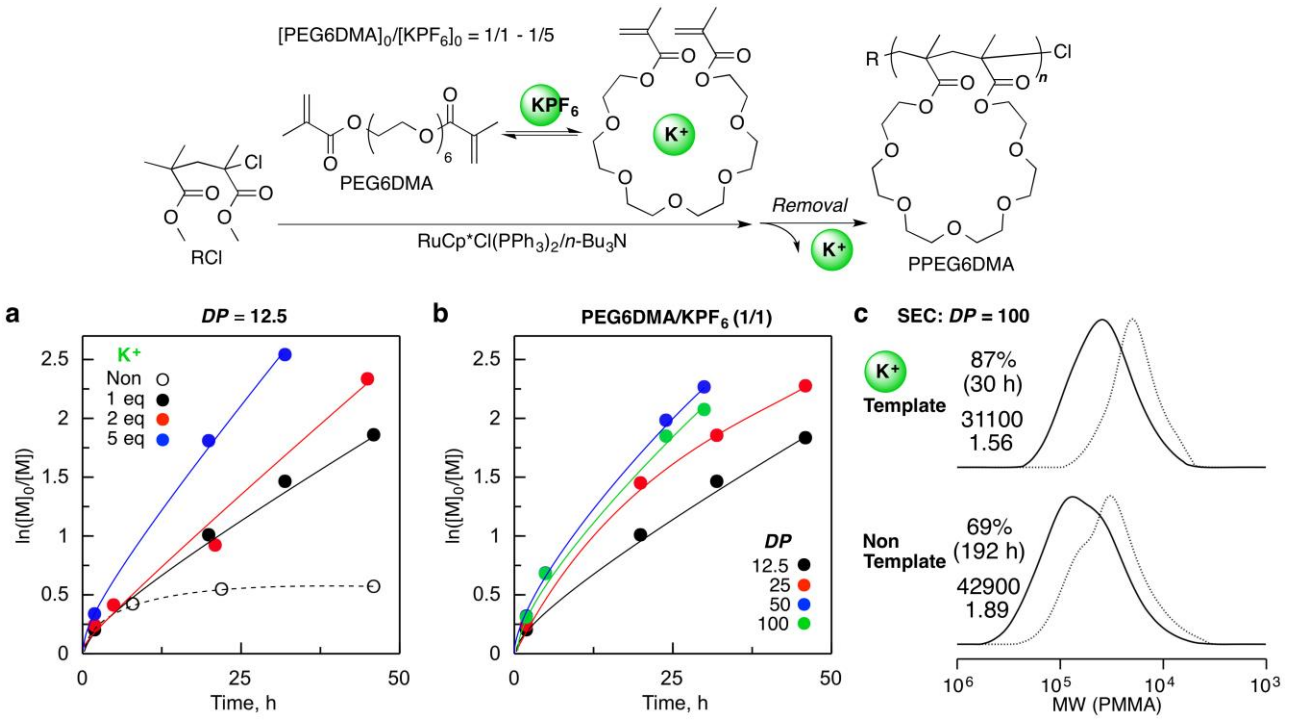

Supplementary Figure S6: Ruthenium-catalyzed cyclopolymerization of PEG6DMA with KPF_6. (**a**) Effects of template amounts to PEG6DMA: $[PEG6DMA]_0/[KPF_6]_0/[H\text{-}(MMA)_2\text{-}Cl\ (RCl)]_0/[RuCp^*Cl(PPh_3)_2]_0/[n\text{-}Bu_3N]_0$ = 25/0, 25, 50, 125/2.0/0.5/20 mM in cyclohexanone at 40 °C. (**b**,**c**) Effects of degree of polymerization (*DP* = $[PEG6DMA]_0/[RCl]_0$): $[PEG6DMA\text{-}KPF_6]_0/[RCl]_0$ = 25/2.0, 50/2.0, 100/2.0, 100/1.0 mM; $[RuCp^*Cl(PPh_3)_2]_0/[n\text{-}Bu_3N]_0$ = 0.5/20 mM in cyclohexanone at 40 °C.

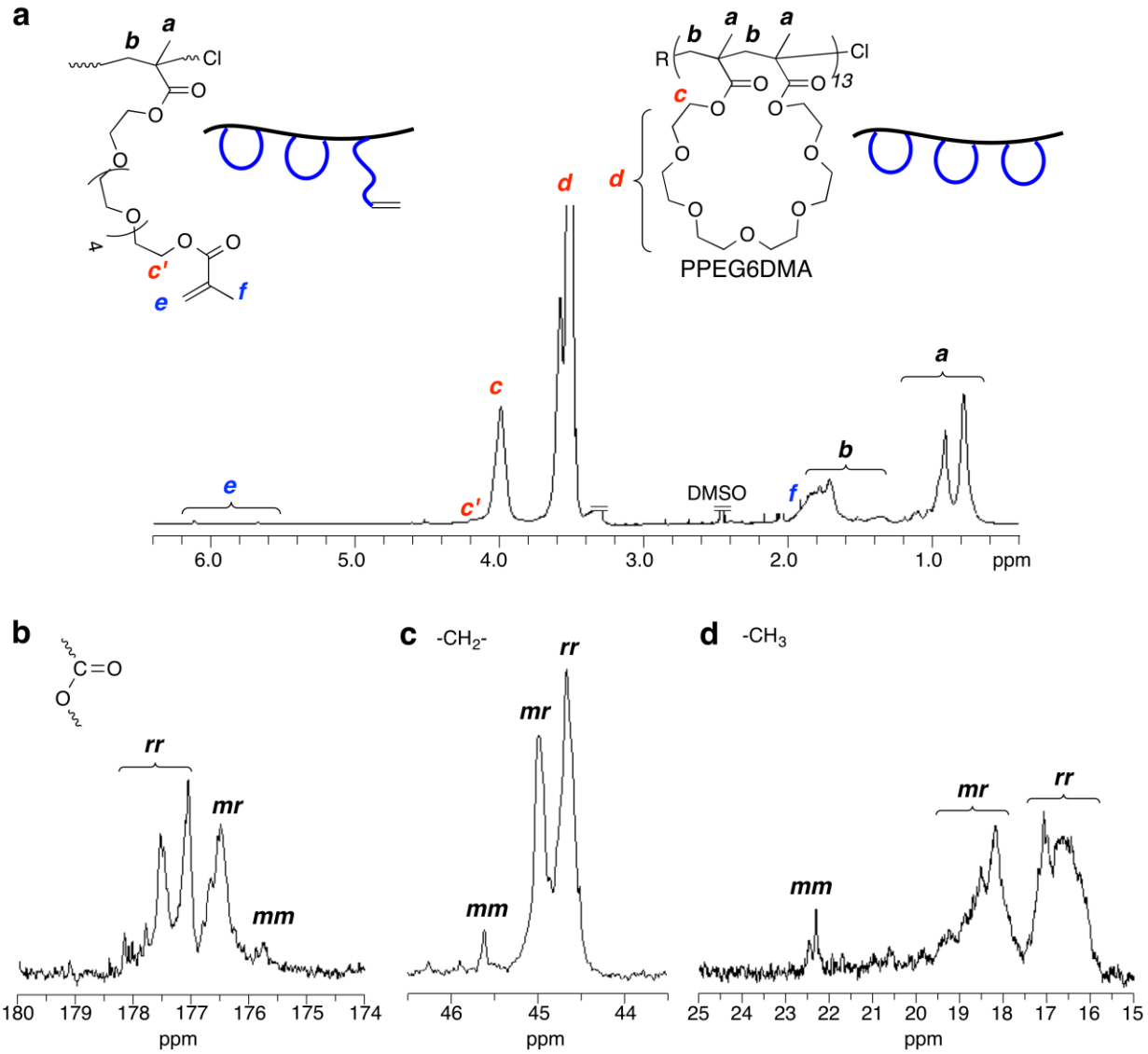

Supplementary Figure S7: ^{1}H and ^{13}C NMR spectra of PPEG6DMA. (a) ^{1}H NMR of a sample (entry 6 in Table S3: M_n = 7500; M_w/M_n = 1.11; CE = 98%) in DMSO-d_6 at room temperature. ^{13}C NMR of a sample (entry 9 in Table S3: M_n = 7900; M_w/M_n = 1.20; olefin = <1%; CE = ~99%) in $CDCl_3$ at 50 ^{o}C: (**b**) carbonyl carbon; (**c**) methylene carbon; (**d**) α-methyl carbon.

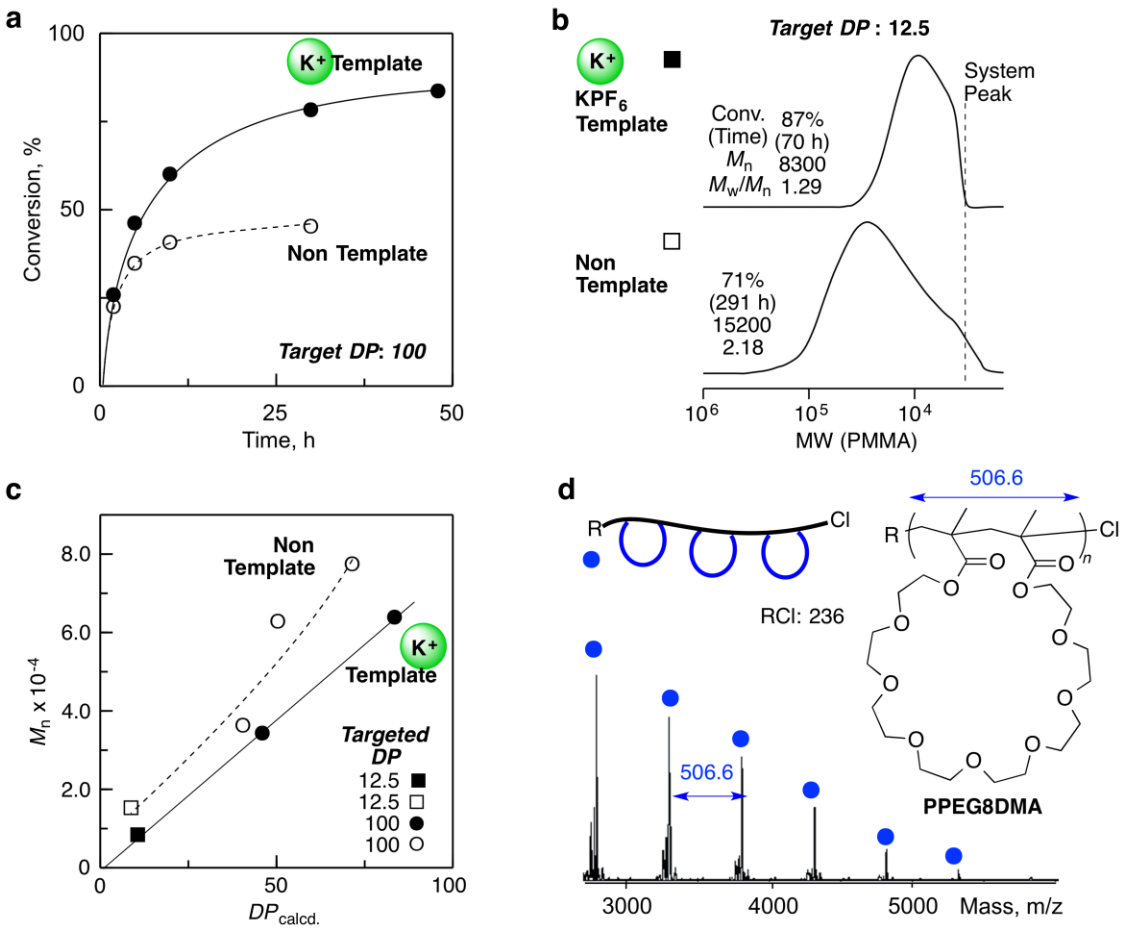

Supplementary Figure S8: Ruthenium-catalyzed cyclopolymerization of PEG8DMA with KPF_6. (**a-c**) $[PEG8DMA]_0/[KPF_6]_0/[H\text{-}(MMA)_2\text{-}Cl\ (RCl)]_0$ = 100/0 or 100/1.0 (*DP* = 100), 25/0 or 25/2.0 (*DP* = 12.5); $[RuCp^*Cl(PPh_3)_2]_0/[n\text{-}Bu_3N]_0$ = 0.5/20 mM in cyclohexanone at 40 °C; $DP_{calcd.}$ = ($[PEG8DMA]_0$ x conv./100 x $[RCl]_0$). (**d**) MALDI-TOF-MS spectrum of PPEG8DMA (*DP* = 12.5).

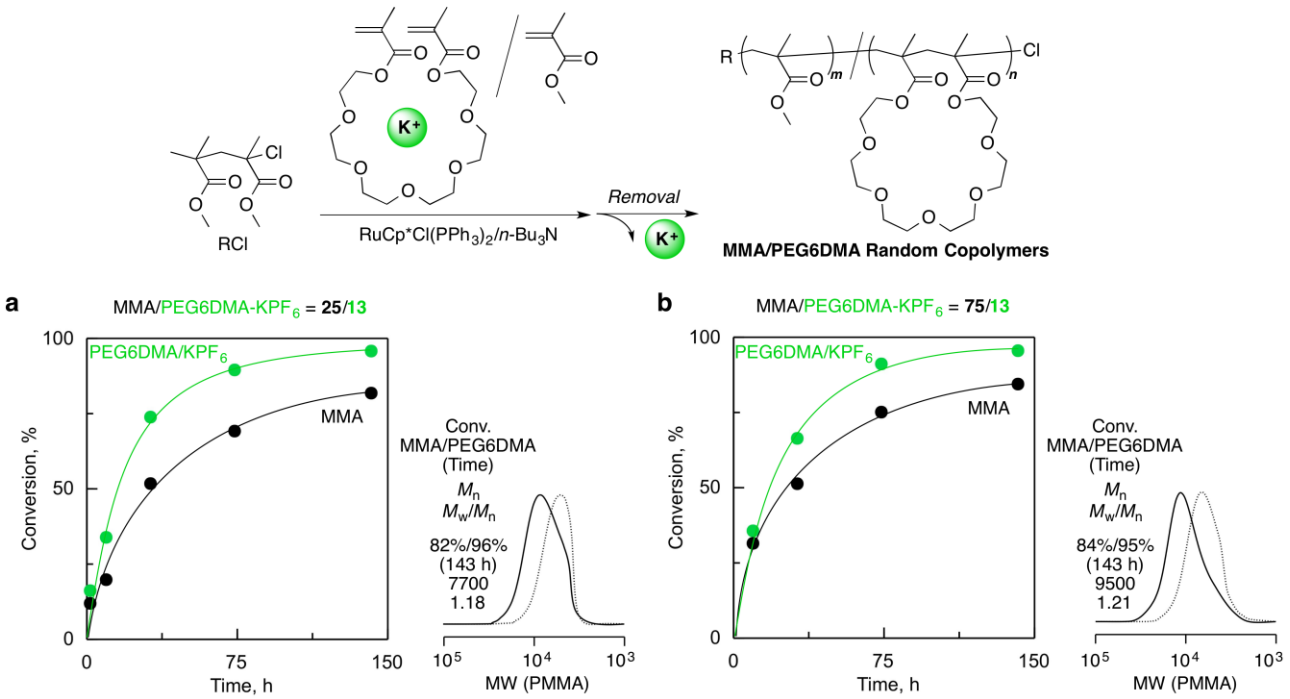

Supplementary Figure S9: Random copolymerization of MMA and PEG6DMA with KPF_6. $[MMA]_0/[PEG6DMA]_0/[KPF_6]_0/[H\text{-}(MMA)_2\text{-}Cl]_0/\ [RuCp^*Cl(PPh_3)_2]_0/[n\text{-}Bu_3N]_0$ = 50 (**a**) or 150 (**b**)/25/50/2.0/0.5/ 20 mM in cyclohexanone at 40 ^oC.

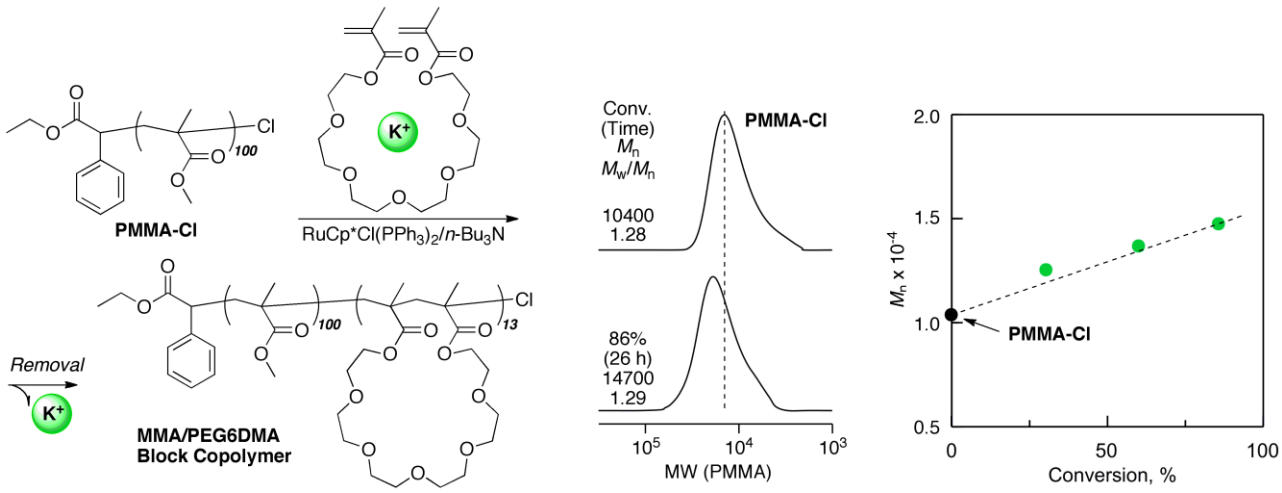

Supplementary Figure S10: Synthesis of a MMA/PEG6DMA (100/13) block copolymer. $[PEG6DMA]_0/[KPF_6]_0/[PMMA\text{-}Cl]_0/[RuCp^*Cl(PPh_3)_2]_0/[n\text{-}Bu_3N]_0$ = 25/50/2.0/0.5/20 mM in cyclohexanone at 40 ^oC.

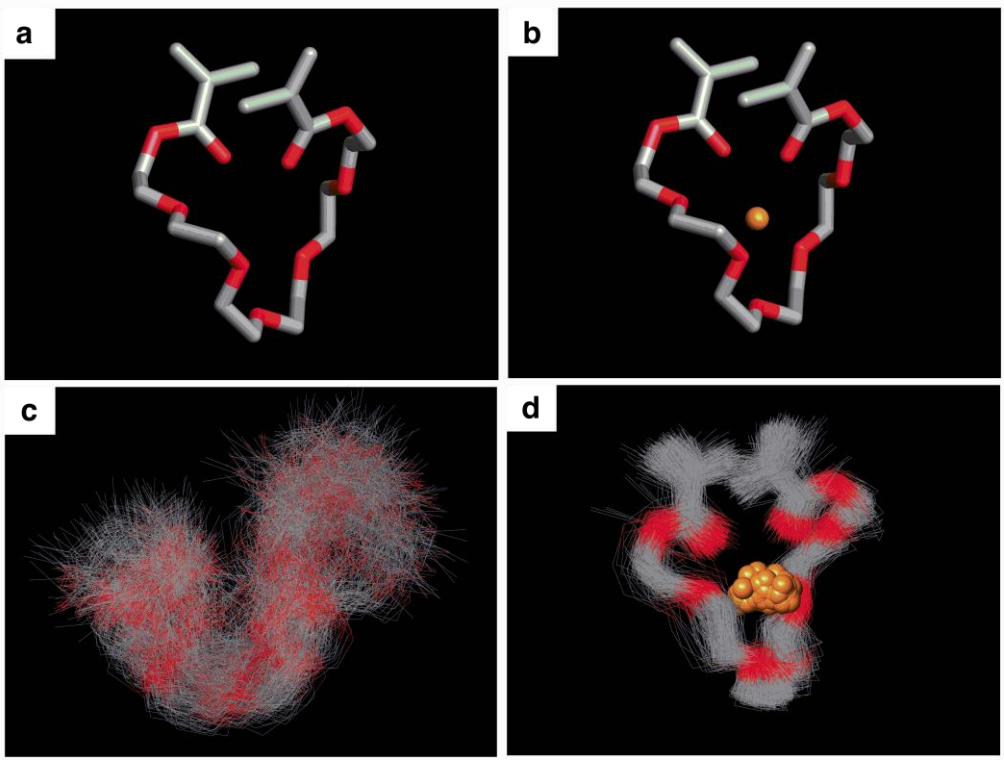

Supplementary Figure S11: Dynamics calculation of PEGnDMA with or without metal cations by MacroModel 9.5 (schrödinger). As an initial structure, the most stable conformation of K^+-template PEG6DMA (**b**) was determined with OPLS 2005 force field. The removal of K^+ from the structure (**b**) provided an initial structure for PEG6DMA (**a**). Dynamics simulation of PEG6DMA and K^+-template PEG6DMA was then carried out for 1000 ps at 300 K with stochastic dynamics method to monitor the distance between two olefin groups. The superimposed structure of 500 conformers for PEG6DMA and that for K^+-template PEG6DMA, sampled every 2 ps during the calculation, were shown in (**c**) and (**d**), respectively. Elements: C grey; O red; K^+ orange.

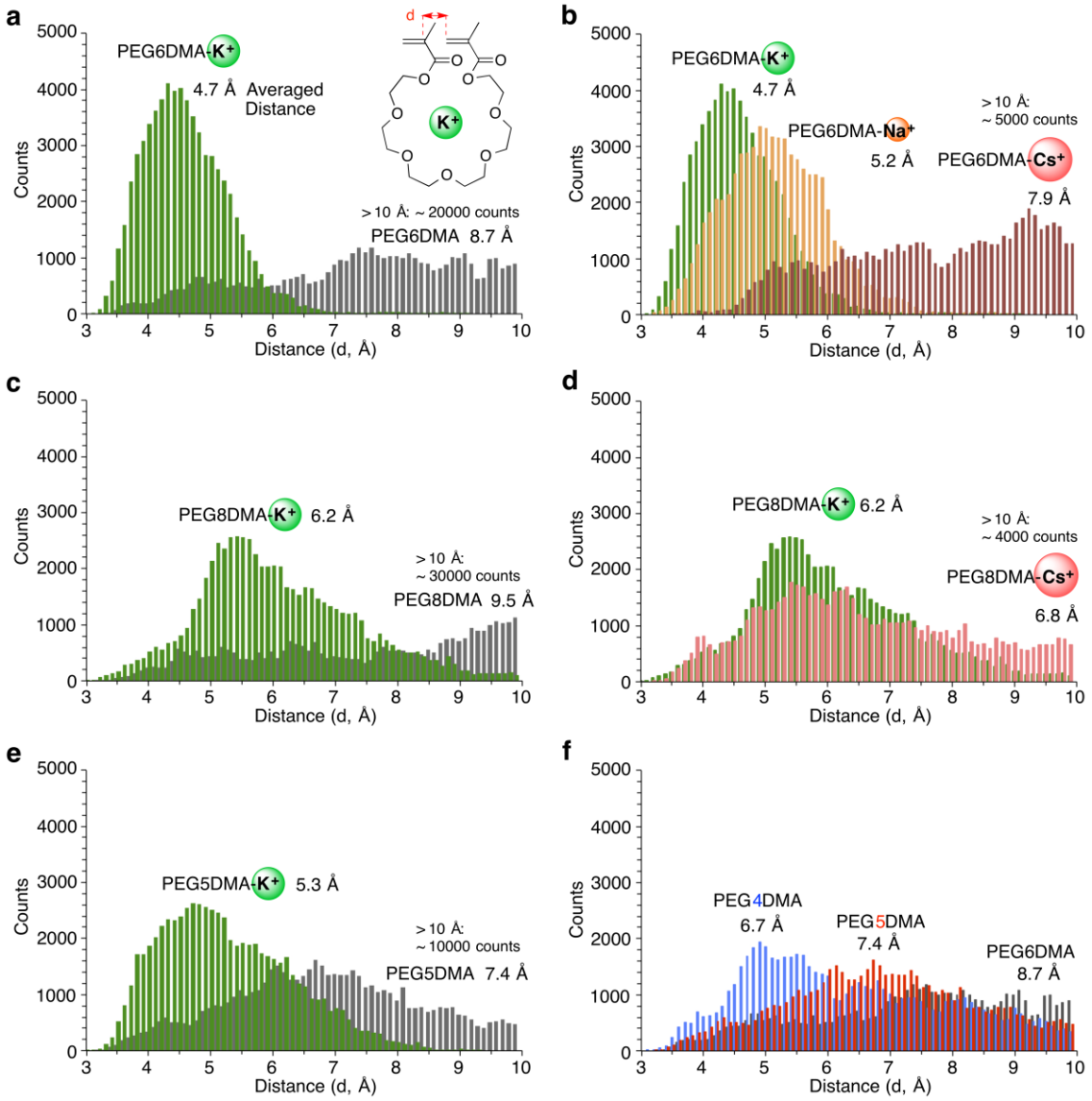

Supplementary Figure S12: Distribution of olefin distance for PEGnDMA with or without metal cations. PEGnDMA-K^+ vs. PEGnDMA [n = 6 (**a**), 8 (**c**), 5 (**e**)]. (**b**) Effects of metal cations (Na^+, K^+, Cs^+) on PEG6DMA. (**d**) Effects of metal cations (K^+, Cs^+) on PEG8DMA. (**f**) Effects of PEG spacer length of PEGnDMAs (n = 4, 5, 6). A K^+ template effectively restricted the change of PEGnDMA conformation to give the averaged olefin distance much smaller than non-template condition. Averaged distance of the two vinyl groups of PEG6DMA decreased according to this order: non (8.7 Å) > Cs^+ (7.9 Å) > Na^+ (5.2 Å) > K^+ (4.7 Å). In contrast, the averaged olefin distance for PEG8DMA with Cs^+ was similar to that with K^+. The position of the two vinyl groups for PEG4DMA was originally closer those for PEG5DMA and PEG6DMA.

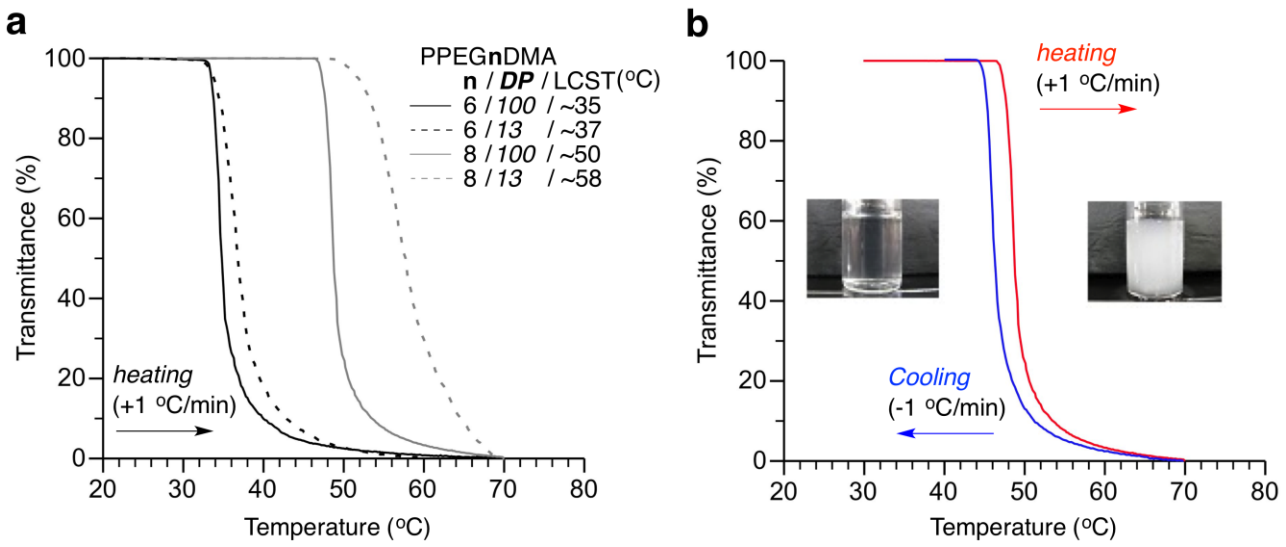

Supplementary Figure S13: Temperature-responsive solubility of PPEGnDMA in water. (**a**) Transmittance of aqueous solutions of PPEGnDMA with different PEG length (n = 6 or 8) and/or *DP* (*100* or *13*) as a function of temperature (heating: 1 °C/min from 20 to 80 °C): [PPEGnDMA] = 1 mg/mL. (**b**) Transmittance of aqueous solution of PPEG8DMA (*DP = 100*) as a function of temperature [heating: 1 °C/min (red line); cooling: -1 °C/min (blue line)]: [PPEG8DMA] = 1 mg/mL.

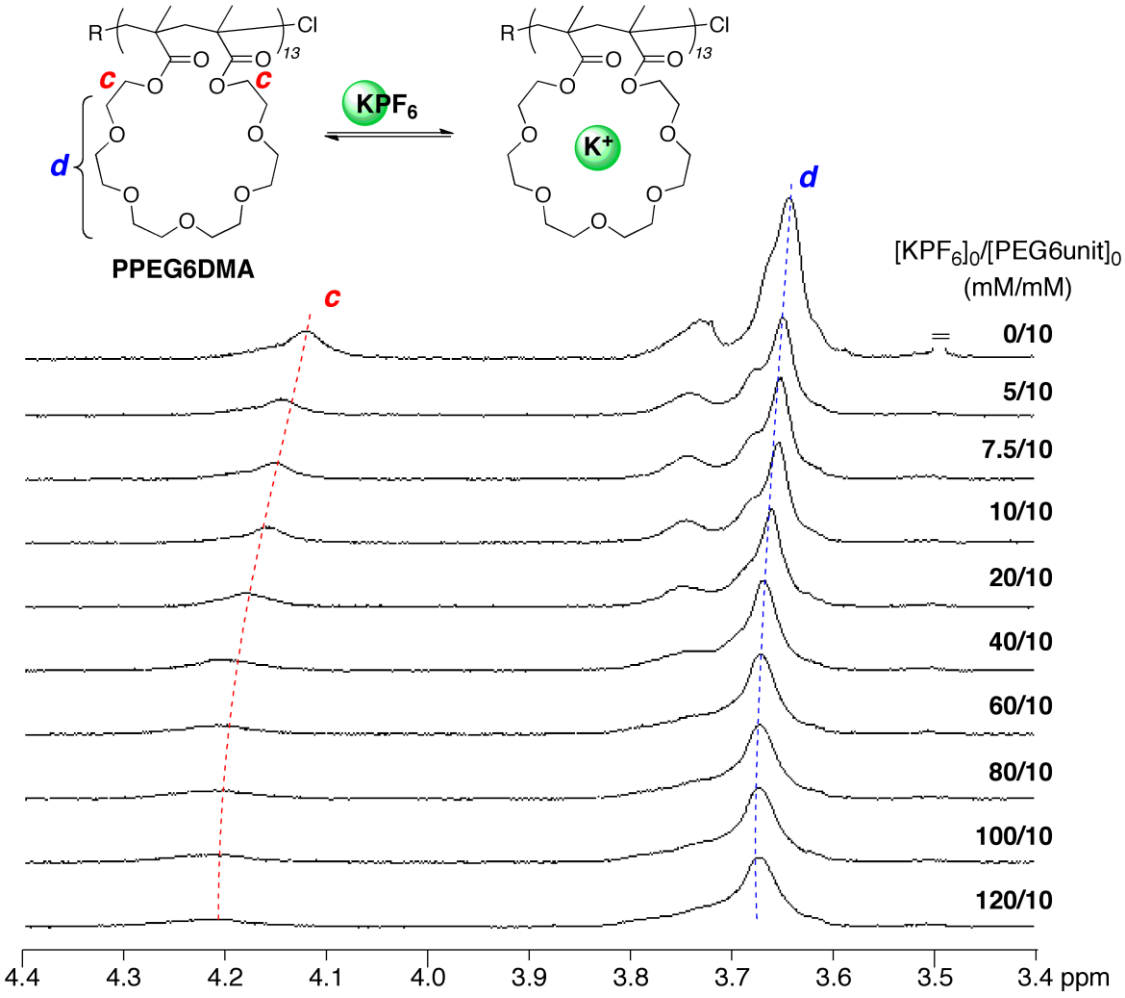

Supplementary Figure S14: ^{1}H NMR titration experiments of PPEG6DMA with KPF_6. [PEG6DMA unit]$_0$/[KPF_6]$_0$ = 10/0 – 120 mM in acetone-d_6 /cyclohexanone (1/1, v/v) at 30 ^{o}C. PPEG6DMA: M_n = 7900, M_w/M_n = 1.2.

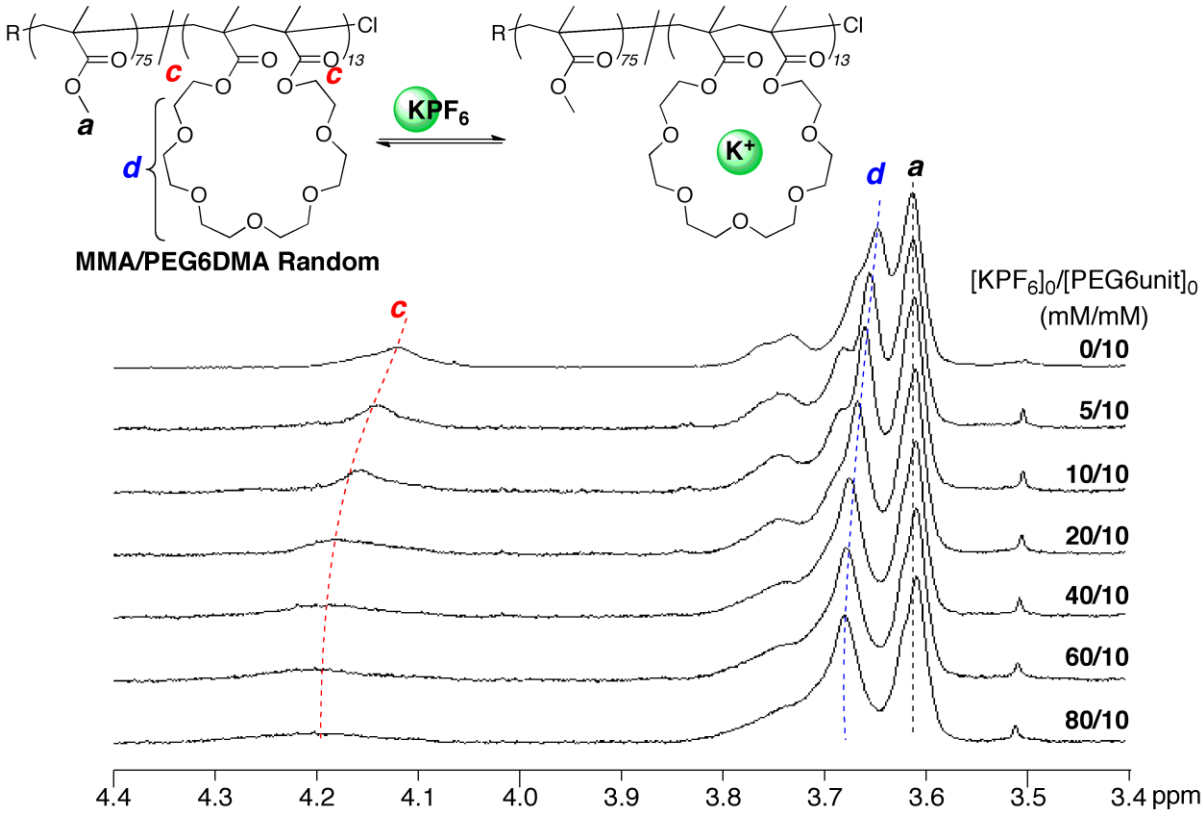

Supplementary Figure S15: ^{1}H NMR titration experiments of a MMA/PEG6DMA (75/13) random copolymer with KPF_6. [PEG6DMA unit]$_0$/[KPF_6]$_0$ = 10/0 – 80 mM in acetone-d_6/cyclohexanone (1/1, v/v) at 30 ^{o}C. MMA/PEG6DMA (75/13) random copolymer: M_n = 9500, M_w/M_n = 1.2.

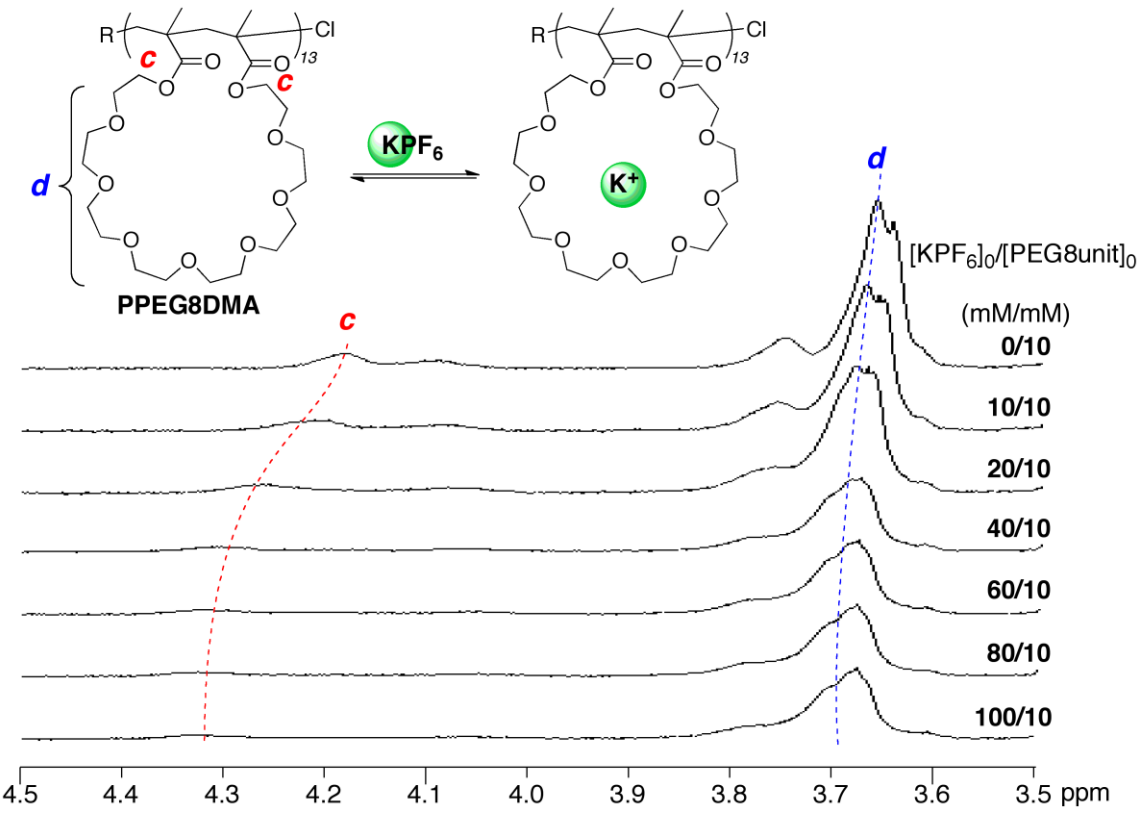

Supplementary Figure S16: ^{1}H NMR titration experiments of PPEG8DMA with KPF_6. $[PEG8DMA\ unit]_0/[KPF_6]_0$ = 10/0 – 100 mM in acetone-d_6/cyclohexanone (1/1, v/v) at 30 ^oC. PPEG8DMA: M_n = 12400, M_w/M_n = 1.3.

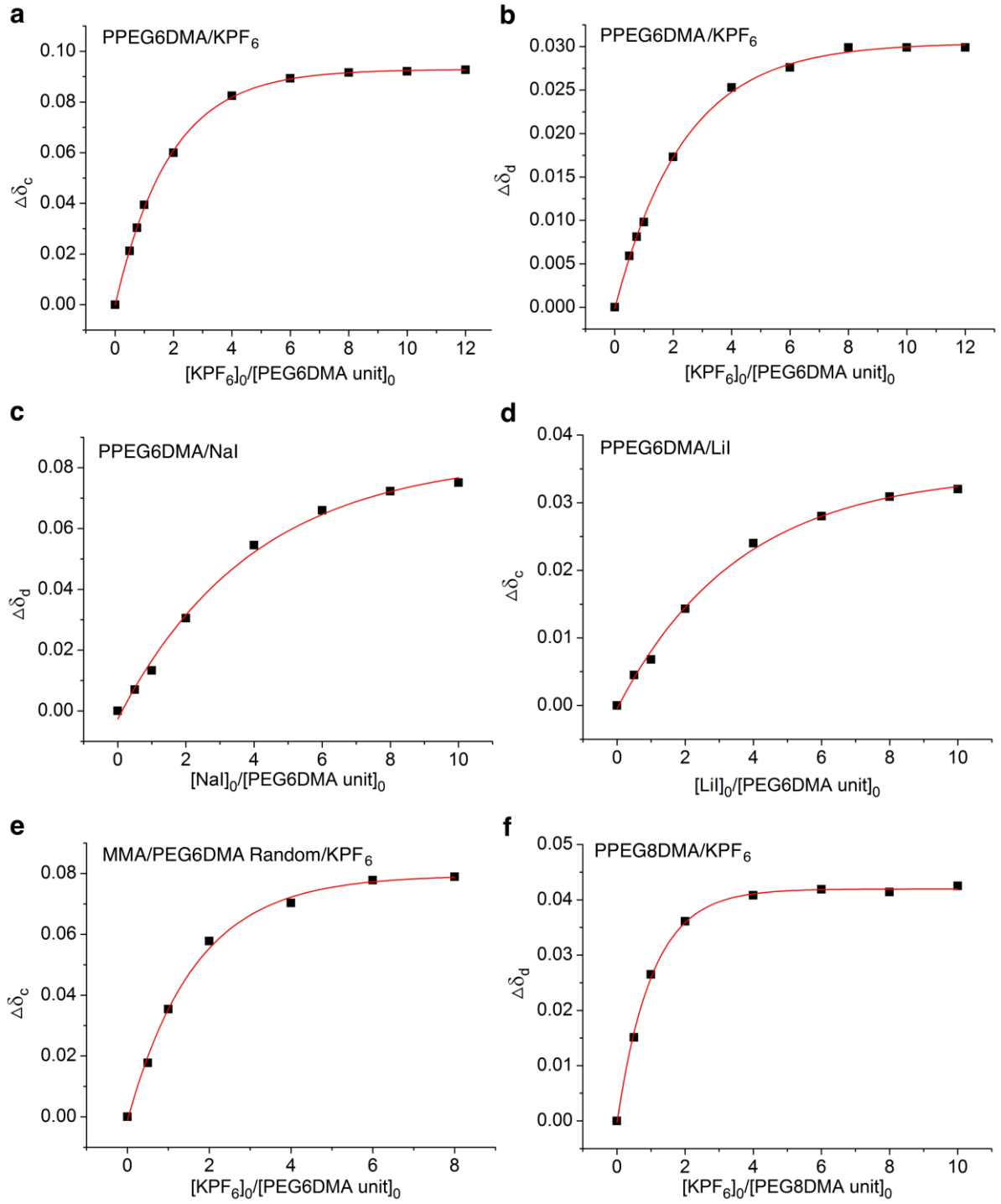

Supplementary Figure S17: Curve fitting of the chemical shift changes for PEG protons of PPEGnDMA with metal cations. Polymer: PPEG6DMA (M_n = 7900, M_w/M_n = 1.2); a MMA/PEG6DMA (75/13) random copolymer (M_n = 9500, M_w/M_n = 1.2); and PPEG8DMA (M_n = 12400, M_w/M_n = 1.3). Condition: [PEGnDMA unit]/[metal cations] = 10/0-120 mM in acetone-d_6/cyclohexanone (1/1, v/v) at 30 ^oC. Peak *c* (**a**) and peak *d* (**b**) for PPEG6DMA with KPF_6. Peaks *d* for PPEG6DMA with NaI (**c**) or LiI (**d**). (**e**) Peak *c* for a MMA/PEG6DMA random copolymer with KPF_6. (**f**) Peak *c* for PPEG8DMA with KPF_6.

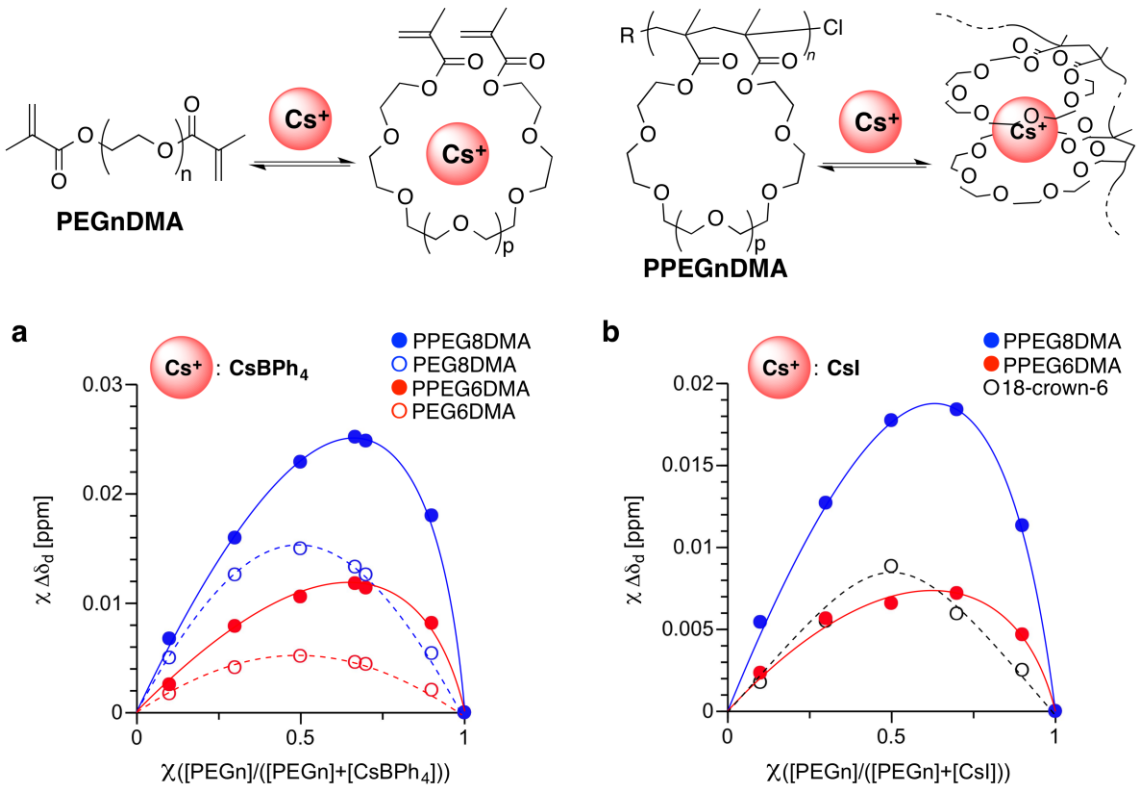

Supplementary Figure S18: Job plots for complexation of PPEGnDMA and Cs cations. (**a**) PPEGnDMA [n = 6 (filled red circle), 8 (filled blue circle)] or PEGnDMA [n = 6 (open red circle), 8 (open blue circle)] with $CsBPh_4$ in acetone-d_6/cyclohexanone (1/1, v/v) at 30 ^{o}C. (**b**) PPEGnDMA [n = 6 (filled red circle), 8 (filled blue circle)] or 18-crown-6 with CsI in CD_3OD at 30 ^{o}C. ^{1}H NMR measurement: $[PEG\ units]_0 + [cation]_0 = 10$ mM.

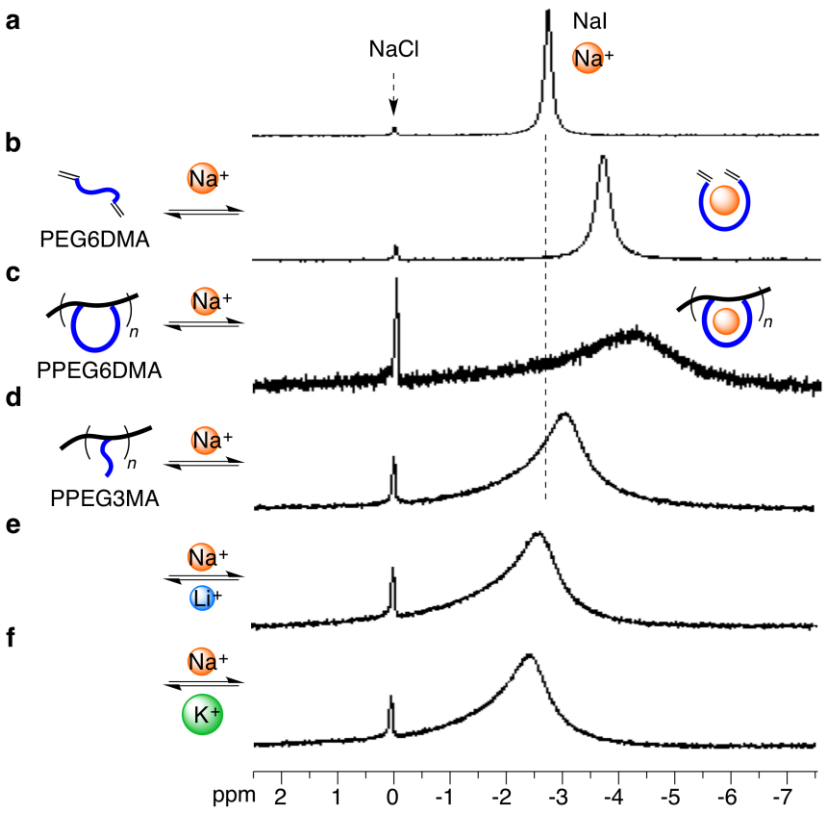

Supplementary Figure S19: Competitive recognition of NaI with PPEG3MA in the presence of other cations. ^{23}Na NMR spectra of NaI alone (**a**) and NaI with PEG6DMA (**b**), PPEG6DMA (**c**), and PPEG3MA (**d**) in cyclohexanone/acetone-d_6 (1/1, v/v) at 30 ^{o}C. ^{23}Na NMR spectra of NaI with PPEG3MA in the presence of LiI (**e**) or KI (**f**) in cyclohexanone/acetone-d_6 (1/1, v/v) at 30 ^{o}C.

Supplementary Table S1: Association Constant of PEGnDMA and Metal Cations[a]

Monomer/Cation	peak	$\subset\delta_1$ (ppm) [b]	$\subset\delta_{max}$ (ppm) [c]	x [d]	K_a (M^{-1}) [d]
PEG6DMA/KPF_6	*c*	0.0214	0.0801	0.267	50
	d'	0.0140	0.0461	0.304	63
	d	0.0203	0.0636	0.319	69
PEG6DMA/NaI	*c*	0.0179	0.0866	0.207	33
	d'	0.0147	0.0779	0.189	29
	d	0.0197	0.0967	0.204	32
PEG5DMA/KPF_6	*c*	0.0047	0.0512	0.092	11
	d'	0.0029	0.0369	0.079	9.3
	d	0.0046	0.0627	0.073	8.5
PEG8DMA/KPF_6	*c*	0.0664	0.0952	0.698	764
	d'	0.0560	0.0774	0.724	954
	d	0.0646	0.0882	0.733	1024

[a] Association constant (K_a) was determined by ^{1}H NMR titration experiments of poly(ethylene glycol) dimethacrylate (PEGnDMA) with metal cations (M^+) and curve fitting of the change in chemical shift of PEG protons (*c*, *c'*, *d*: assigned in Supplementary Figure S2) with Origin 8.5 (Supplementary Figure S3).

[b] $\subset\delta_1 = \delta_{PEGnDMA/Cation\ (1/1)} - \delta_{PEGnDMA}$. $\delta_{PEGnDMA/Cation\ (1/1)}$: chemical shift (ppm) of PEG6DMA in the presence of cation ($[cation]_0/[PEGnDMA]_0$ = 10/10 mM). $\delta_{PEGnDMA}$: chemical shift (ppm) of PEGnDMA alone.

[c] $\subset\delta_{max} = \delta_{max} - \delta_{PEGnDMA}$: determined by curve fitting of the chemical shift change ($\subset\delta_c$, $\subset\delta_{d'}$, $\subset\delta_d$) with Origin 8.5.

[d] K_a for the complexation (PEGnDMA-M^+: HG) between PEGnDMA (host: H) and M^+ (guest: G) is represented by the following equations.

$$K_a = [HG]/[H][G] \quad (S1)$$

$$[H] = [H]_0 (1-x) \quad (S2)$$

$$[G] = [G]_0 (1-x) \quad (S3)$$

$$x = [HG]/[H]_0 = (\delta_{PEGnDMA/Cation\ (1/1)} - \delta_{PEGnDMA})/(\delta_{max} - \delta_{PEGnDMA}) = \subset\delta_1/\subset\delta_{max} \quad (S4),$$

where [H], [G], and [HG] are concentration of host, guest, and complex, respectively, at equilibrium, $[H]_0$ and $[G]_0$ are initial concentration of host and guest, respectively, and x is the ratio of complex ([HG]) at equilibrium over initial host ($[H]_0$).

Thus, equation (S5) is derived from Equation (S1)-(S4) with $[H]_0 = [G]_0$ (= 1.0 x 10^{-2} M) to give K_a.

$$K_a\ (M^{-1}) = x/[H]_0(1-x)^2 = 100x/(1-x)^2 \quad (S5)$$

Supplementary Table S2: T_1 **Values of Carbons for PEG6DMA**

peak	T_1 (s) [a]	T_1 (K^+)(s) [b]	T_1 (K^+)/T_1
a	4.26	3.75	0.88
b	2.07	1.32	0.64
c	1.98	0.94	0.47
d	1.93	0.74	0.38

[a] T_1 values of carbons for hexaethylene glycol dimethacrylate (PEG6DMA, peaks: assigned in Supplementary Figure S4) determined by ^{13}C NMR: [PEG6DMA] = 120 mM in acetone-d_6/cyclohexanone (1/1, v/v) at 30 ^oC.

[b] T_1 values of carbons for PEG6DMA in the presence of KPF_6: [PEG6DMA]/[KPF_6] = 120/240 mM in acetone-d_6/cyclohexanone (1/1, v/v) at 30 ^oC.

Supplementary Table S3: Cation Template-Assisted Cyclopolymerization[a]

Entry	PEG (**n**)	*DP*	M^+	PEG/M^+	Time (h)	Conv.[b] (%)	M_n[c]	M_w/M_n[c]	CE (%)[d] (olefin/linking)
1	4	12.5	-	1/0	96	63	3600	1.08	99 (1/-)
2	5	12.5	-	1/0	122	85	3800	1.22	- (30/+)
3	6	12.5	$LiPF_6$	1/2	51	80	5200	1.09	85 (15/-)
4	6	12.5	$NaPF_6$	1/2	46	62	8800	1.15	93 (7/-)
5	6	12.5	$CsBPh_4$	1/1	144	78	5700	1.10	85 (15/-)
6	8	100	-	1/0	248	72	77400	4.39	- (10/+)
7	8	100	KPF_6	1/1	48	84	63800	2.20	97 (3/-)

[a] $[PEGnDMA]_0/[M^+]_0/[H\text{-}(MMA)_2\text{-}Cl\ (RCl)]_0/[RuCp^*Cl(PPh_3)_2]_0/[n\text{-}Bu_3N]_0$ = 25 or 100/0, 25, 50, 100/1 or 2/0.5/20 mM in cyclohexanone at 40 °C; *DP* = $[PEG6DMA]_0/[RCl]_0$ = 25/2 or 100/1 (mM/mM) = 12.5 or 100; $M^+ = LiPF_6$, $NaPF_6$, KPF_6, $CsBPh_4$.

[b] Determined by ^1H NMR with tetralin as an internal standard.

[c] M_n and M_w/M_n of final products: determined by SEC in DMF (10 mM LiBr) with PMMA standard calibration.

[d] Cyclization efficiency (CE), olefin (pendant olefin content), and linking (intermolecular linking of chains) for initial products (conv. = <30%). Olefin content: determined by ^1H NMR with the following equation: $100[4\boldsymbol{e}/(\boldsymbol{c} + \boldsymbol{c'})]$ (%) (peaks: assigned in Supplementary Figure S7). Linking: confirmed by MALDI-TOF-MS and SEC (high MW) (+: observed; -: not observed). CE for non-linking samples was calculated from the following: CE (%) = 100 – olefin.

Supplementary Table S4: T_1 Values of PEG Carbons[a]

entry	sample	T_1 (s)
1	PEG6DMA	1.93
2	PEG6DMA-KPF_6 (PEG6/K = 1/2)	0.74
3	PPEG4DMA[b]	0.48
4	PPEG5DMA[b]	0.48
5	PPEG6DMA[b]	0.51
6	PPEG6DMA[b]-KPF_6 (PEG6/K = 1/1)	0.27
7	PPEG8DMA[b]	0.68
8	PPEG*8.5*MA[c]	1.68

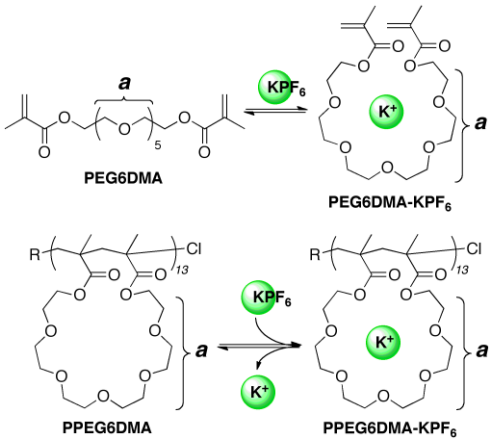

[a] T_1 values of carbons (***a***) of PEG segments: determined by ^{13}C NMR in acetone-d_6/cyclohexanone (1/1, v/v) at 30 ^{o}C: [sample] = 100 mg/mL.

[b] PPEG4DMA (entry 3), PPEG5DMA (entry 4), PPEG6DMA (entry 5, 6), and PPEG8DMA (entry 7) correspond to entry 9, 10, 3, and 12 in Table 1 in main text.

[c] M_n = 9100, M_w/M_n = 1.12.

Supplementary Table S5: Association Constant (K_a) of PPEGnDMA and Metal Cations [a]

Monomer/Cation	peak	$\subset\delta_1$ (ppm) [b]	$\subset\delta_{max}$ (ppm) [c]	x [d]	K_a (M^{-1}) [d]
PPEG6DMA/KPF_6	*c*	0.0394	0.0929	0.424	128
	d	0.0098	0.0304	0.322	70
PPEG6DMA/NaI	*d*	0.0133	0.0835	0.159	23
PPEG6DMA/LiI	*c*	0.0068	0.0337	0.202	32
	d	0.0047	0.0571	0.082	10
MMA/PEG6DMA	*c*	0.0354	0.0794	0.446	145
Random/ KPF_6	*d*	0.0144	0.0340	0.424	128
PEG8DMA/KPF_6	*c*	0.0791	0.1967	0.421	113
	d	0.0265	0.0420	0.631	463

[a] Association constant (K_a) was determined by ^{1}H NMR titration experiments of poly(poly(ethylene glycol) dimethacrylate) (PPEGnDMA) with metal cations (M^+) and curve fitting of the change in chemical shift of the PEG protons (*c, d*: assigned in Supplementary Figures S14-16) with Origin 8.5 (Supplementary Figure S17).

[b] $\subset\delta_1 = \delta_{PPEGnDMA/Cation\ (1/1)} - \delta_{PPEGnDMA}$. $\delta_{PEGnDMA/Cation\ (1/1)}$: chemical shift (ppm) of PEG6DMA with a cation ($[cation]_0/[PEGnDMA]_0$ = 10/10 mM). $\delta_{PEGnDMA}$: chemical shift (ppm) of PEGnDMA alone.

[c] $\subset\delta_{max} = \delta_{max} - \delta_{PPEGnDMA}$: determined by curve fitting of the chemical shift change ($\subset\delta_c$, $\subset\delta_d$) with Origin 8.5.

[d] K_a for the complexation (cycloPEG-M^+: HG) between a cycloPEG unit in PPEGnDMA (host: H) and M^+ (guest: G) is represented by equations S1 to S5.

Supplementary Methods

PEGnDMA synthesis. PEGnDMA (n = 4, 5, and 8) were synthesized by the esterification of poly(ethylene glycol) with methacryloyl chloride, similarly to PEG6DMA shown in the main text.

PEG4DMA. ^{1}H NMR [500 MHz, acetone-d_6, r.t., δ = 2.05 ppm (acetone)]: δ 6.07 (m, olefin, 2H), 5.62 (m, olefin, 2H), 4.24 (t, *J* = 4.8 Hz, 4H, -COOC*H*$_2$CH$_2$O-), 3.72 (t, *J* = 4.8 Hz, 4H, -COOCH$_2$C*H*$_2$O-), 3.62-3.58 (m, 8H, -OC*H*$_2$C*H*$_2$O-), 1.92 (m, 6H, -CC*H*$_3$). ^{13}C NMR [125 MHz, acetone-d_6, r.t., δ = 206.5 ppm (acetone)]: δ 168.0, 138.0, 126.3, 72.0, 70.3, 65.3, 19.1. ESI-MS m/z ([M + Na]$^+$): calcd. for $C_{16}H_{26}O_7Na$ 353.2, found 353.2.

PEG5DMA. ^{1}H NMR [500 MHz, acetone-d_6, r.t., δ = 2.05 ppm (acetone)]: δ 6.07 (m, olefin, 2H), 5.62 (m, olefin, 2H), 4.24 (t, *J* = 4.9 Hz, 4H, -COOC*H*$_2$CH$_2$O-), 3.72 (t, *J* = 4.9 Hz, 4H, -COOCH$_2$C*H*$_2$O-), 3.62-3.57 (m, 12H, -OC*H*$_2$C*H*$_2$O-), 1.92 (m, 6H, -CC*H*$_3$). ^{13}C NMR [125 MHz, acetone-d_6, r.t., δ = 206.5 ppm (acetone)]: δ 168.0, 138.0, 126.3, 72.0, 70.3, 65.3, 19.1. ESI-MS m/z ([M + Na]$^+$): calcd. for $C_{18}H_{30}O_8Na$ 397.2, found 397.2.

PEG8DMA. ^{1}H NMR [500 MHz, acetone-d_6, r.t., δ = 2.05 ppm (acetone)]: δ 6.09 (m, olefin, 2H), 5.62 (m, olefin, 2H), 4.26 (t, *J* = 4.9 Hz, 4H, -COOC*H*$_2$CH$_2$O-), 3.73 (t, *J* = 4.9 Hz, 4H, -COOCH$_2$C*H*$_2$O-), 3.63-3.57 (m, 24H, -OC*H*$_2$C*H*$_2$O-), 1.93 (m, 6H, -CC*H*$_3$). ^{13}C NMR [125 MHz, acetone-d_6, r.t., δ = 206.5 ppm (acetone)]: δ 168.0, 138.0, 126.3, 72.0, 70.3, 65.3, 19.2. ESI-MS m/z ([M + Na]$^+$): calcd. for $C_{24}H_{42}O_{11}Na$ 529.2, found 529.2.

Polymerization. Cation template-assisted living radical cyclopolymerization of PEGnDMA (n = 4, 5, and 8) and living radical polymerization of PEGnMA (n = 3, *8.5*) were carried out by syringe technique under argon in baked glass tubes equipped with a three-way stopcock, similarly to PPEG6DMA shown in the main text.

PPEG4DMA (*DP* = 12.5) SEC (DMF, 0.01 M LiBr): M_n = 7200 g/mol; M_w/M_n = 1.19. ^{1}H NMR [500 MHz, $CDCl_3$, δ = 7.26 ($CHCl_3$)]: δ 6.1, 5.6 (olefin), 4.2-4.0 (-COOC*H*$_2$CH$_2$O-), 3.8-3.5 (-OC*H*$_2$C*H*$_2$O-), 2.1-1.3 (-C*H*$_2$CCH$_3$), 1.3-0.8 (-CC*H*$_3$). ^{13}C NMR [125 MHz, $CDCl_3$, δ = 77.0 ($CHCl_3$)]: δ 178.2-175.8 (C=O), 71.3-70.5 (-O*C*H$_2$*C*H$_2$O-), 69.0-68.5 (-COOCH$_2$*C*H$_2$O-), 64.8-63.8 (-COO*C*H$_2$CH$_2$O-), 55.6-52.0 (-CH$_2$*C*(CH$_3$)CO-), 46.1-44.8 (-*C*H$_2$C(CH$_3$)CO-), 23.0-16.1 (-*C*H$_3$).

PPEG5DMA (*DP* = 12.5) SEC (DMF, 0.01 M LiBr): M_n = 8300 g/mol; M_w/M_n = 1.21. ^{1}H NMR [500 MHz, $CDCl_3$, δ = 7.26 ($CHCl_3$)]: δ 6.1, 5.6 (olefin), 4.2-4.0 (-COOC*H*$_2$CH$_2$O-), 3.8-3.5 (-OC*H*$_2$C*H*$_2$O-), 2.1-1.4 (-C*H*$_2$CCH$_3$), 1.3-0.8 (-CC*H*$_3$). ^{13}C NMR [125 MHz, $CDCl_3$, δ = 77.0 ($CHCl_3$)]: δ 178.2-175.8 (C=O), 71.3-70.5 (-O*C*H$_2$*C*H$_2$O-), 69.1-68.6 (-COOCH$_2$*C*H$_2$O-), 64.9-64.0 (-COO*C*H$_2$CH$_2$O-), 55.7-52.0 (-CH$_2$*C*(CH$_3$)CO-), 46.1-44.8 (-*C*H$_2$C(CH$_3$)CO-), 23.0-16.4 (-*C*H$_3$).

PPEG8DMA (*DP* = 12.5) SEC (DMF, 0.01 M LiBr): M_n = 8300 g/mol; M_w/M_n = 1.29. ^{1}H NMR [500 MHz, $CDCl_3$, δ = 7.26 ($CHCl_3$)]: δ 6.1, 5.6 (olefin), 4.2-4.0 (-COOC*H*$_2$CH$_2$O-), 3.8-3.5

(-OCH_2CH_2O-), 2.1-1.3 (-CH_2CCH$_3$), 1.3-0.8 (-CCH_3). ^{13}C NMR [125 MHz, $CDCl_3$, δ = 77.0 ($CHCl_3$)]: δ 178.2-175.7 (C=O), 71.2-70.4 (-OCH_2CH_2O-), 68.9-68.5 (-COOCH$_2$CH_2O-), 64.4-63.8 (-COOCH_2CH$_2$O-), 55.5-52.0 (-CH$_2$C(CH$_3$)CO-), 45.9-44.8 (-CH$_2$C(CH$_3$)CO-), 23.1-16.6 (-CH$_3$).

MMA/PEG6DMA (75/13) Random copolymer RuCp*Cl(PPh_3)$_2$ (0.005 mmol, 4.0 mg) was placed in a 30 mL glass tube. Into the tube, cyclohexanone (8.22 mL), tetralin (0.1 mL), a 400 mM toluene solution of *n*-Bu_3N (0.2 mmol, 0.5 mL), MMA (1.5 mmol, 0.16 mL), a 372/744 mM cyclohexanone solution of PEG6DMA/KPF_6 (0.25/0.5 mmol, 0.67 mL), and a 57.6 mM toluene solution of H-(MMA)$_2$-Cl (0.02 mmol, 0.35 mL) were added sequentially in this order at 25 °C under argon. The total volume of the reaction mixture was thus 10 mL. The tube with the mixture was placed in an oil bath at 40 °C. In predetermined intervals, a small portion of the reaction mixture was sampled and cooled to -78 °C to terminate the reaction. The conversion of MMA and PEG6DMA was determined by ^{1}H NMR with tetralin as an internal standard. After 143 h (MMA/PEG6DMA conversion = 84/95 %), the quenched reaction mixture was evaporated to dryness under reduced pressure. The resulting crude was first fractionated by preparative SEC in DMF and then dialyzed in water with a regenerated cellulose membrane (Spectra/Por® 7; MWCO 1000) for 5 day. The inner purified solution was evaporated to dryness under reduced pressure to give a MMA/PEG6DMA random copolymer (Figure S10). SEC (DMF, 0.01 M LiBr): M_n = 9500 g/mol; M_w/M_n = 1.21. ^{1}H NMR [500 MHz, DMSO-d_6, δ = 2.49 (DMSO)]: δ 4.1-3.9 (-COOCH_2CH$_2$O-), 3.7-3.5 (-OCH_2CH_2O-, -OCH_3), 2.1-1.4 (-CH_2CCH$_3$), 1.2-0.7 (-CCH_3).

MMA/PEG6DMA (100/13) Block copolymer The block copolymer was prepared by the following two steps: 1) living radical polymerization of MMA with Ru(Ind)Cl(PPh_3)$_2$/*n*-Bu_3N/ECPA to give a chlorine-capped macroinitiator (PMMA-Cl: M_n = 10400 g/mol; M_w/M_n = 1.29); 2) KPF_6-assisted cyclopolymerization of PEG6DMA with Ru(Ind)Cl(PPh_3)$_2$/*n*-Bu_3N/PMMA-Cl (Figure S11). SEC (DMF, 0.01 M LiBr): M_n = 14700 g/mol; M_w/M_n = 1.29. ^{1}H NMR [500 MHz, DMSO-d_6, δ = 2.49 (DMSO)]: δ 7.3-7.1 (aromatic), 4.1-3.9 (-COOC<u>H</u>$_2$CH$_2$O-, -COOC<u>H</u>$_2$CH$_3$), 3.8-3.5 (-OCH$_2$CH$_2$O-), 2.1-1.4 (-C<u>H</u>$_2$CCH$_3$), 1.3-0.7 (-CH$_2$CC<u>H</u>$_3$). CE = ~100%. PEGMA/MMA contents: 102/11 (NMR); 103/11 (calcd.). M_n (NMR, α) = 15000 g/mol.

PPEG3MA (M_n = 25200 g/mol; M_w/M_n = 1.14) was synthesized by living radical polymerization of PEG3MA with Ru(Ind)Cl(PPh_3)$_2$, *n*-Bu_3N, and H-(MMA)$_2$-Cl in toluene at 80 °C.[47]

PPEG*8.5*MA (M_n = 30000 g/mol; M_w/M_n = 1.23) and **PPEG*4*MA** (M_n = 12000 g/mol; M_w/M_n = 1.09) was synthesized by living radical polymerization of PEG*8.5*MA with RuCp*Cl(PPh_3)$_2$, *n*-Bu_3N, and H-(MMA)$_2$-Cl in cyclohexanone at 40 °C.[48]

Supplementary References

47. Terashima, T., Mes, T., De Greef, T. F. A., Gillissen, M. A. J., Besenius, P., Palmans, A. R. A., Meijer, E. W. Single-chain folding of polymers for catalytic systems in water. *J. Am. Chem. Soc.* **133**, 4742-4745 (2011).

48. Yoda, H., Nakatani, K., Terashima, T., Ouchi, M., Sawamoto, M. Ethanol-mediated living radical homo- and copolymerizations with Cp*-ruthenium catalysts: active, robust, and universal for functionalized methacrylates. *Macromolecules* **43**, 5595-5601 (2010).